termis.

Tissue Engineering
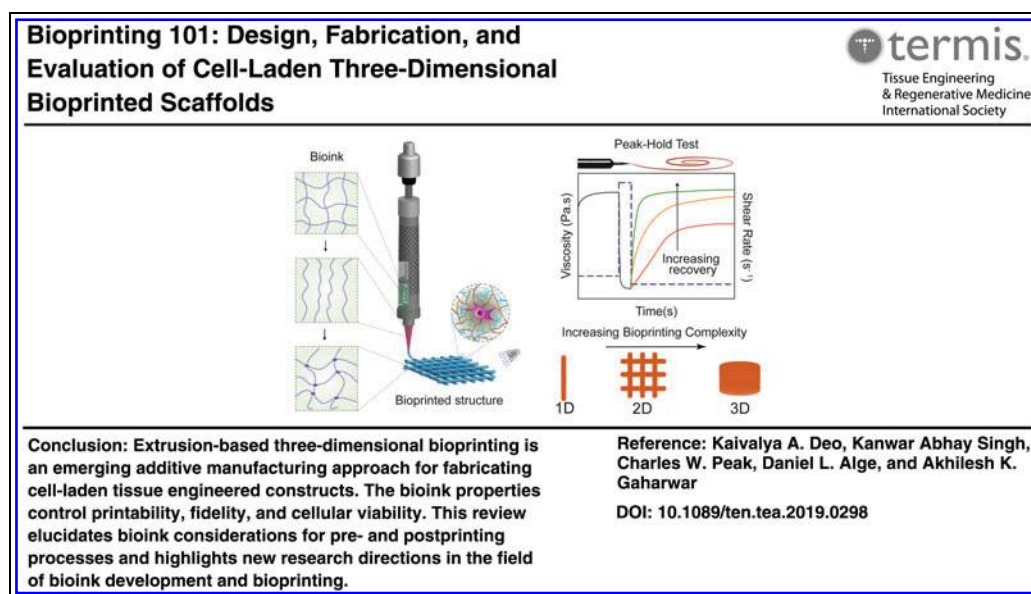& Regenerative Medicine
International Society

ORIGINAL ARTICLE

Bioprinting 101: Design, Fabrication, and Evaluation of Cell-Laden 3D Bioprinted Scaffolds

Kaivalya A. Deo, BS,[1] Kanwar Abhay Singh, MS,[1] Charles W. Peak, PhD,[1]
Daniel L. Alge, PhD,[1,2] and Akhilesh K. Gaharwar, PhD[1–3]

3D bioprinting is an additive manufacturing technique that recapitulates the native architecture of tissues. This is accomplished through the precise deposition of cell-containing bioinks. The spatiotemporal control over bioink deposition permits for improved communication between cells and the extracellular matrix, facilitates fabrication of anatomically and physiologically relevant structures. The physiochemical properties of bioinks, before and after crosslinking, are crucial for bioprinting complex tissue structures. Specifically, the rheological properties of bioinks determines printability, structural fidelity, and cell viability during the printing process, whereas postcrosslinking of bioinks are critical for their mechanical integrity, physiological stability, cell survival, and cell functions. In this review, we critically evaluate bioink design criteria, specifically for extrusion-based 3D bioprinting techniques, to fabricate complex constructs. The effects of various processing parameters on the biophysical and biochemical characteristics of bioinks are discussed. Furthermore, emerging trends and future directions in the area of bioinks and bioprinting are also highlighted.

Graphical abstract

Color images are available online.

[1]Biomedical Engineering and [2]Materials Science and Engineering, College of Engineering, Texas A&M University, College Station, Texas.
[3]Center for Remote Health Technologies and Systems, Texas A&M University, College Station, Texas.

Keywords: 3D bioprinting, bioink, hydrogels, additive manufacturing, tissue models, organ printing

Impact Statement

Extrusion-based 3D bioprinting is an emerging additive manufacturing approach for fabricating cell-laden tissue engineered constructs. This review critically evaluates bioink design criteria to fabricate complex tissue constructs. Specifically, pre- and post-printing evaluation approaches are described, as well as new research directions in the field of bioink development and functional bioprinting are highlighted.

Introduction

ADDITIVE MANUFACTURING IS a layer-by-layer fabrication process to construct complex three-dimensional (3D) objects.[1] 3D bioprinting, an emerging category of additive manufacturing, focuses on precise deposition of cell-laden hydrogel bioinks to construct tissue engineered structures (Fig. 1a).[2] A multitude of 3D bioprinting techniques have been developed, including laser-assisted printing,[3,4] inkjet printing,[5,6] and extrusion-based printing.[7,8] Among these different approaches, extrusion-based 3D bioprinting has become a popular technique as hydrogel precursors with low-shear viscosities ($>10^2$ Pa·s) can be used for bioprinting.[9–11] In addition, 3D bioprinting is also being explored for designing a range of tissue types for regenerative medicine (Fig. 1b).[12]

One of the primary components of 3D bioprinting is hydrogel bioinks. Hydrogels are water swollen polymeric networks that can be engineered to control various cellular functions such as adhesion, spreading, proliferation, and differentiation.[13–19] Hydrogels exhibit cytocompatibility and are extensively used to design cell-laden constructs.[13,14] Recent developments in hydrogel chemistries, reinforcement approaches, and crosslinking methods have expanded the applications of
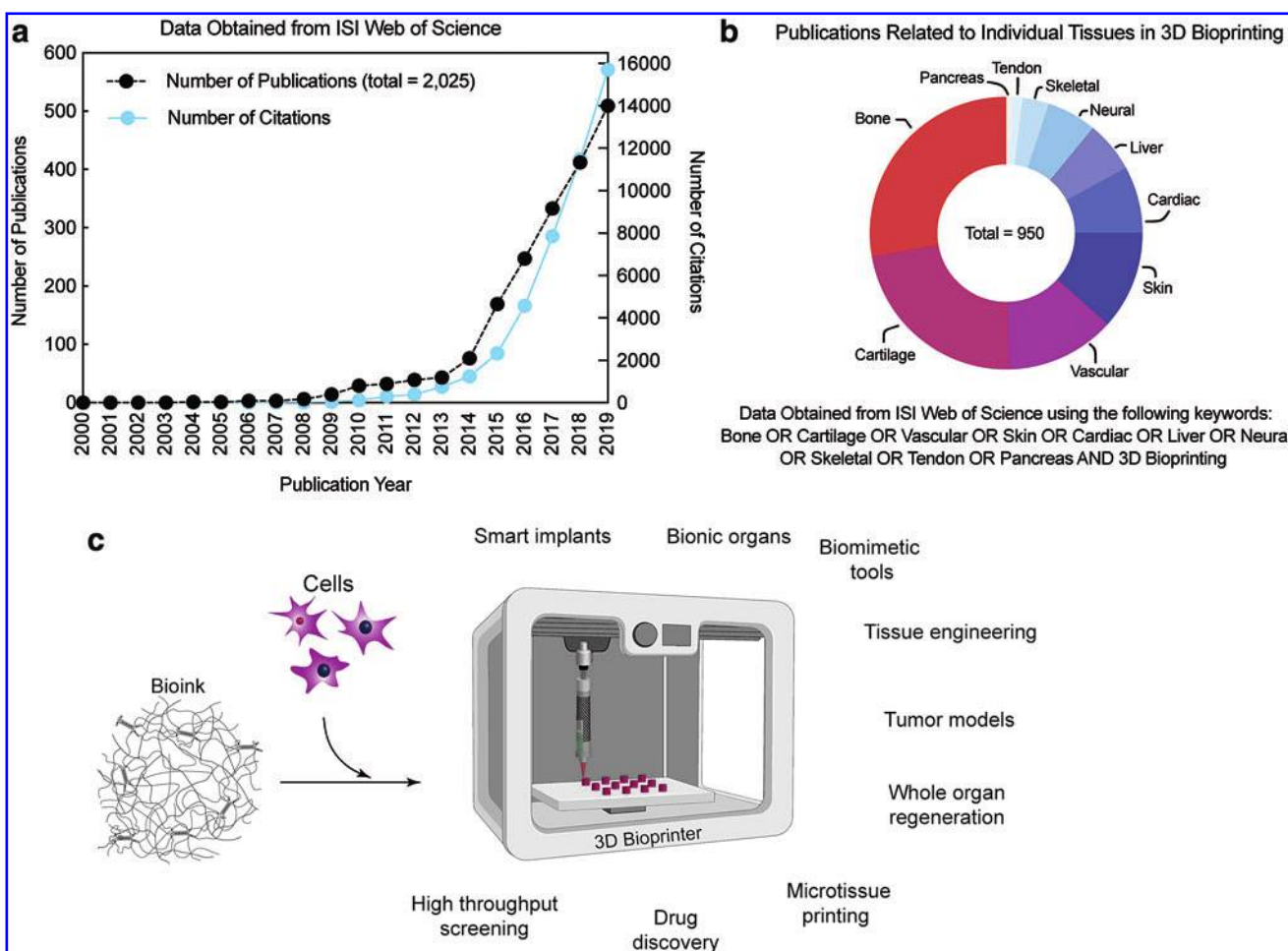

FIG. 1. Trends in 3D bioprinting. **(a)** Exponential research growth in the field of 3D bioprinting. Data obtained from ISI Web of Science using "3D bioprinting." **(b)** Publications in the field of 3D bioprinting focusing on various tissue types. Data obtained from ISI Web of Science, specifically looking at "3D bioprinting" and "bone/cartilage/vascular/skin/cardiac/liver/neural/skeletal/tendon or pancreas" (February 2020). **(c)** Various applications of 3D bioprinting are explored in the field of pharmaceutics, regenerative medicine and biomedical devices. 3D, three-dimensional. Color images are available online.

3D bioprinting to pharmaceutics, regenerative medicine, and biomedical devices (Fig. 1c). Thus, it is imperative to understand the fundamental relationships between hydrogel formulation, biophysical characteristics, and cellular interactions in 3D microenvironments.[20–22] Furthermore, bioink characterization in terms of swelling, degradation, and flow properties will provide insight about the performance of bioinks and 3D printed structures in physiological conditions.[23,24]

In this review, we discuss biophysical and biochemical characteristics of bioinks and their relationship to the extrusion-based 3D bioprinting process. Specifically, bioink characteristics at different stages of the bioprinting process are highlighted. We attempt to elucidate mechanical properties, cell-material interplay and the effects of processing parameters on cellular viability in the bioprinting process. Finally, promising new research directions in the field of bioprinting are also summarized.

Extrusion-Based 3D Bioprinting

In extrusion-based 3D bioprinting, a nozzle continuously extrudes the bioink filament and enables deposition in predefined geometries. During the extrusion process, the bioink should possess low viscosity to prevent possible clogging of the extrusion tips (needle) as well as protect cells from excessive fluid shear stress. Upon deposition on the printer bed, the bioink should undergo rapid solidification to maintain the deposited shape.[25,26] The resolution through extrusion bioprinting is generally between 50 and 1000 μm.[27,28] The process of extrusion-based bioprinting involves considerations at three different stages of bioprinting.

The crucial bioink characteristics at preextrusion stage include precursor viscosity, cell distribution, and biocompatibility.[29] The critical bioink attribute at mid-extrusion stage considers shear stress minimization through plug flow behavior, and postextrusion stage includes physiological stability postcrosslinking of 3D printed structures (Fig. 2a).[7,30,31] Careful control of biomaterial chemistry determines stiffness and dictates the processing capability of the bioink. The potential to deposit high cell densities, matching the physiological structure, is a major advantage of extrusion-based bioprinting.[32,33] Hence, designing appropriate bioinks is crucial for obtaining 3D prints with relevant resolution, fidelity, cell density, and other essential properties.[34]

Bioinks and the biofabrication window

Bioinks for extrusion-based 3D bioprinting need to withstand high shear forces during the extrusion process and recover rapidly thereafter. Typically, polymer formulations that stabilize rapidly, such as gelatin methacryloyl (Gel-MA)[35,36] or alginate,[37,38] have been used. To design bioinks for 3D bioprinting, the concept of the biofabrication window has been traditionally utilized. The biofabrication window describes the trade-offs between printability and cell viability within the constructs (Fig. 2b). It details the compromise in bioink design that is made to devise bioinks with suboptimal printability while maintaining cellular activity.[39] Advanced bioinks use numerous strategies to elevate printability and cellular compatibility simultaneously. Such advanced bioink formulations are designed with shear-thinning abilities, which modulate viscosity during bioprinting process and allow the bioink to regain its orig-

inal viscosity postextrusion. Advanced bioinks also protect the encapsulated cells without compromising the printability or print fidelity.[40]

Bioprinting considerations

A range of biophysical and biochemical attributes of bioinks can influence 3D printability. These properties include shear-thinning, recoverability, gelation kinetics, biocompatibility, and biodegradation. Before printing, computer aided design (CAD) files are used to design the construct to be printed. CAD software provides an array of tools to create complex and anatomically relevant structures. CAD files are subsequently converted to g-code, which communicates the desired printing path and parameters (i.e., speed, location, infill) to the 3D printer.[41] The bioprinting speed is regulated and is usually between 700 mm·s^{-1} and 10 μm·s^{-1}.[42,43] Subsequently, bioinks are loaded into extrusion barrels for bioprinting. Mechanical properties, such as viscosity and shear-thinning ability of bioinks, are critical to improve cell viability when exposed to the printing stresses make it possible to extrude the material with minimal applied stress.[44] The usual viscosities of bioinks for extrusion-based bioprinting are between 30 and 6×10^7 mPa·s.[45,46]

Once loaded, bioprinting commences, depositing cell-laden bioinks onto the printer bed. Crosslinking chemistry determines the ability of the hydrogel to form a stable structure.[31,47] Biomechanical considerations of the printed constructs include elastic moduli and mechanical integrity.[48,49] Throughout the printing process, coordinating cell-material interactions, maintaining appropriate rheological characteristics, and maintaining a sterile microenvironment govern the success of the 3D bioprinting process.[50,51] Extrusion-based bioprinting is commonly successful in ensuring long-term high cell viability (~80–90%) in the 3D printed constructs.[52–54] Biochemical considerations of the bioprinted structures include degradability, cell-instructive matrix remodeling, and extracellular matrix (ECM) production (Fig. 2c).[55,56]

Throughout different stages of the bioprinting process, various techniques can be used to measure performance and efficacy. For example, shear rate sweeps can determine if a material has potential to be injectable, and cytotoxicity assays indicate if a material has favorable interactions with cells.[57–59] The proceeding sections will examine the various approaches used to characterize and quantify the utility bioinks for fabricating intricate, complex geometries.

Bioink Design and Preprinting Considerations

3D bioprinting of hydrogel bioinks involves more complex design criteria compared to typical fabrication techniques. For example, bioinks (hydrogel precursors) must be transported through a needle and be able to retain a deposited shape upon extrusion. Appropriate polymer selection is essential to maintain viability of encapsulated cells and achieve the necessary mechanical requirements for 3D printing.[50]

Polymer selection

Bioink composition should support high viability of encapsulated cells and shield cells from shear stress during
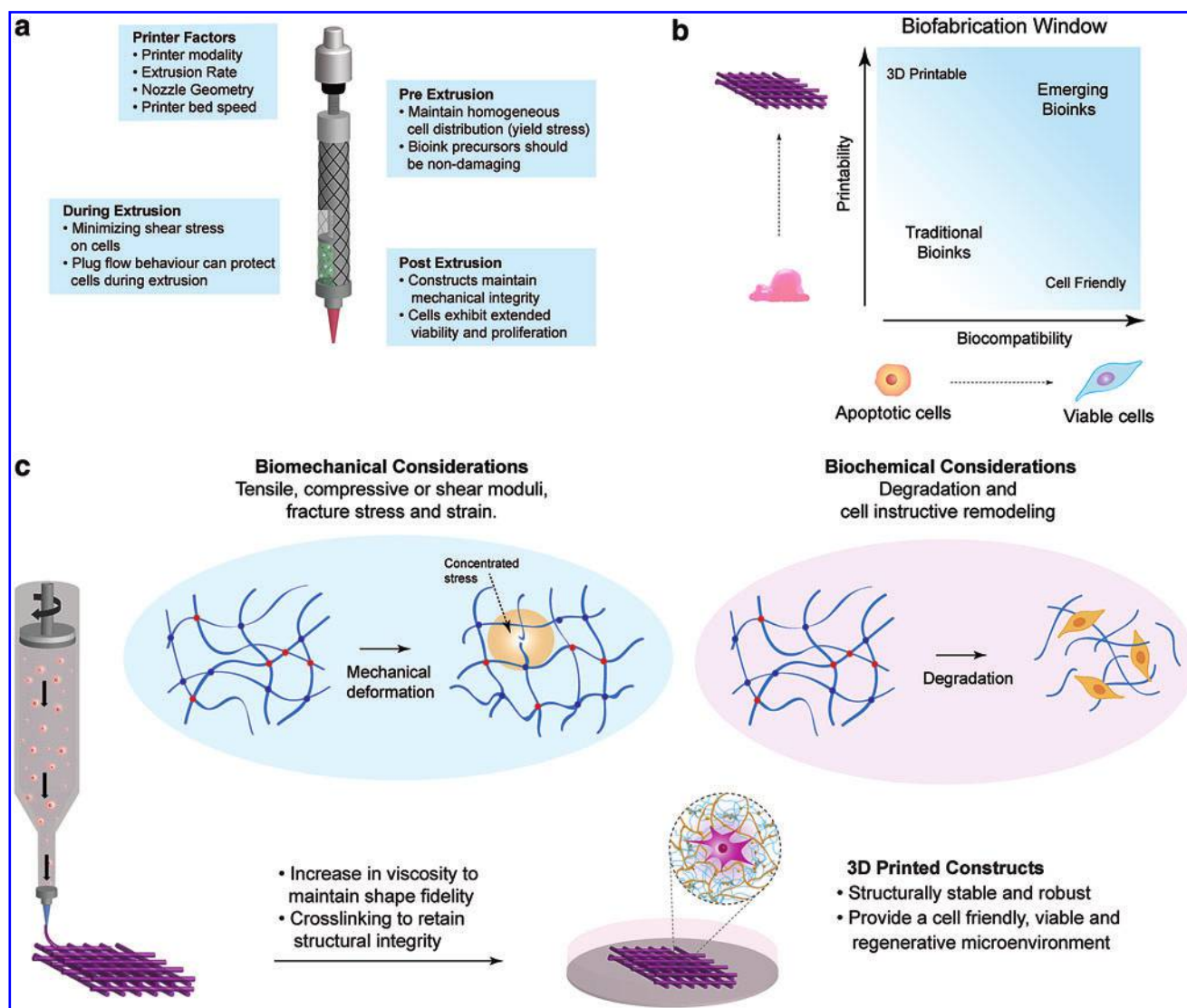
FIG. 2. Considerations for extrusion-based 3D bioprinting. **(a)** Optimizing various printer modalities and pre, mid and post extrusion factors for ensuring favorable properties of the 3D bioprinted constructs. **(b)** Biofabrication window illustrating the trade-off between printability and biocompatibility required to make acceptable bioinks. **(c)** Biomechanical and biochemical considerations of the 3D bioprinted architectures. Coordinating cell–material interactions, mechanical properties of the materials and maintaining cellular viability governs 3D bioprinting proficiency. ECM, extracellular matrix; GAG, glycosaminoglycan; UV, ultraviolet. Color images are available online.

extrusion.[50,60–64] Molecular weight and crosslinking density remain the two most critical physical characteristics that influence cell behavior, regardless of the polymer used.[63,64] Naturally derived polymers, such as gelatin and alginate, have well characterized crosslinking mechanisms and mechanical properties (as a crosslinked hydrogel).[65–68] Naturally derived polymers often exhibit high molecular weights, while synthetic polymers have custom molecular weights.[69,70] However, natural polymers, such as gelatin or GelMA present integrin-binding motifs, facilitating strong bioink–cell interactions. Gelatin with different "bloom strength" reflects the average molecular weight of the polymer. Higher bloom strength indicates formation of stiffer gels. Conversely, synthetic polymers, such as poly(ethylene glycol) (PEG), permit for finely tuned molecular weights ranging from <500 to >1,000,000 Da, which can be leveraged to control mesh size and nutrient diffusion.

Due to the chemical formula ($-CH_2-CH_2-O-$) of the PEG backbone, it is often considered a biologically inert "blank slate" polymer that will interact minimally with cells and the body.[71] However, PEG must be chemically modified to crosslink and form stable hydrogels. Both dimethacrylate and diacrylate PEG have been among the most widely studied model hydrogels.[72] Nuclear magnetic resonance spectroscopy or attenuated total reflectance can be used to verify the terminal end groups of the polymer and molecular weight of the polymer. Overall, bioinks must meet the needs of being able to mechanically deform and reform while also providing an environment for cell proliferation. Achieving a synergistic balance of all the properties is required to maintain printability with active cellular viability and proliferation.[73]

Polymer selection is also influenced by the type of functionalities desired. Molecular weight influences cell

behavior due to the amount of swelling a hydrogel may undergo, resulting in nutrient supplementation and waste removal.[74] Matrix degradability is another factor that plays a significant role in polymer selection.[39,75] Natural polymers derivatives, such as GelMA, contains degradation sites sensitive to matrix metalloproteinases (MMPs). MMPs allow natural cleaving of ECM components permitting cells to remodel and degrade the matrix.[76,77] The end-groups of the polymers determine the crosslinking mechanism that must be used. Acrylate end groups have historically been common as they provide a facile method (ultraviolet curing) for

creation of covalent crosslinks. Similarly, thiol end groups are also involved in unique crosslinking such as thiol-ene click chemistry[78] and thiol-nanoparticle vacancy driven gelation.[79] Some of the common polymer types utilized, their crosslinking approaches and desired functionalities are summarized (Fig. 3a).

Polymer dispersity index (PDI) is another important factor affecting the overall bioink properties. Polymer molecular weight is critical to control bioink flow characteristics and the resulting mechanical and biocompatibility properties.[80] Having low PDI suggests that the polymer is similar
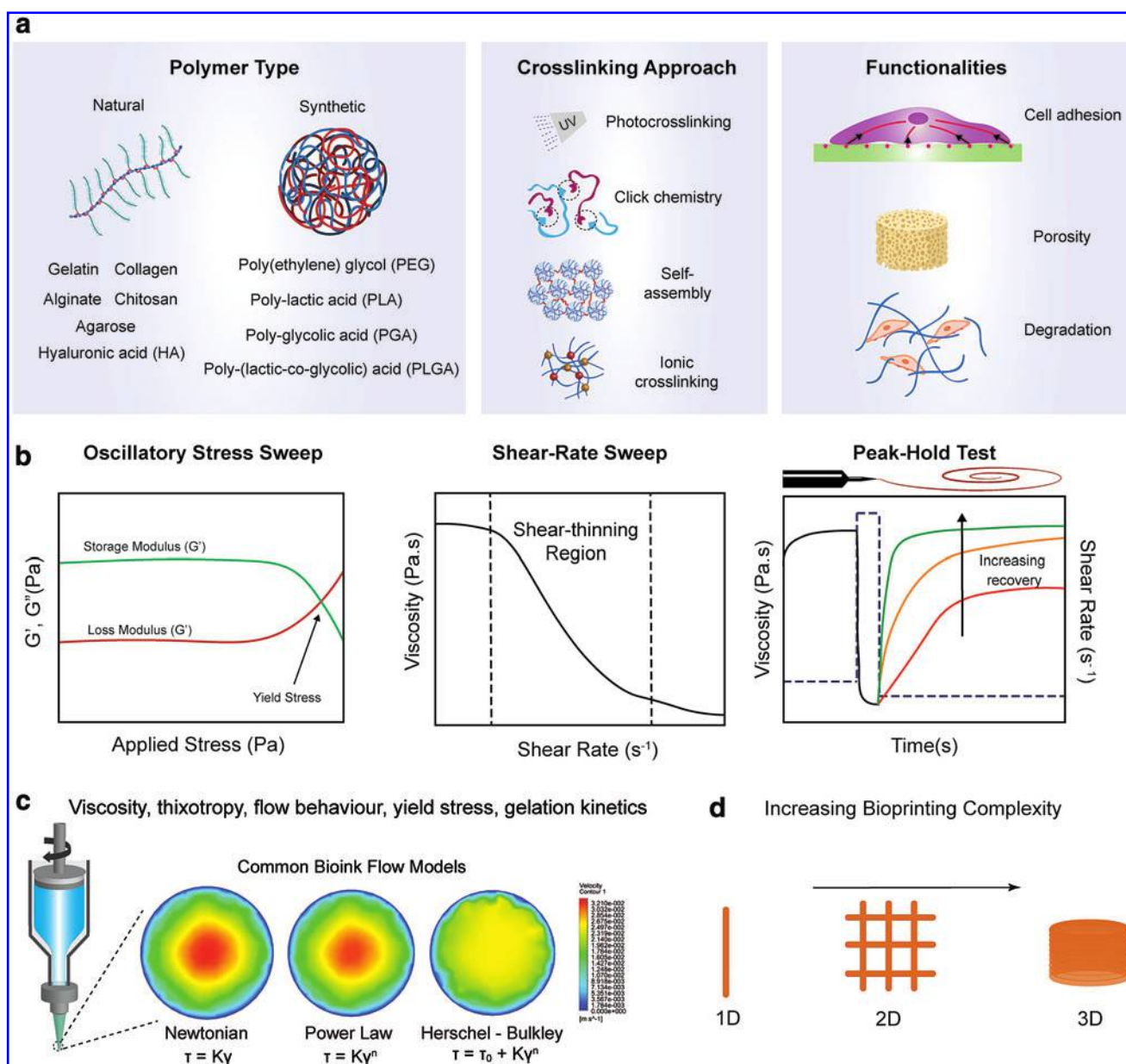

FIG. 3. Preprinting considerations. **(a)** Polymer selection is crucial in designing bioink with tunable performance. Type of polymer, crosslinking mechanisms and desired functionalities are important parameters which can be controlled to achieve enhanced cellular viability and material properties. **(b)** Rheological characterization is important to predict the utility of a bioink for 3D bioprinting. Oscillatory stress-sweep, peak-hold test, and shear rate sweep experiments are important to determine printability of bioink. **(c)** The modeling of flow behavior provides distribution of stress within the bioink during the printing process. **(d)** Increasing bioprinting complexity also requires maintaining high shape fidelity for superior bioprinting and cellular proliferation in the constructs. 1D, one-dimensional; 2D, two-dimensional. Color images are available online.

TABLE 1. COMMON POLYMERS, VISCOSITIES, AND CROSSLINKING MECHANISM FOR BIOINKS

Polymer	Concentration	Crosslinking mechanism	Viscosity range (Pa·s)	Reference
Methacrylated hylaronic acid/ methacrylated gelatin	6–12%	UV	0.1–10,000	212
PEG-DA + Laponite	10% PEG-DA, 4% Laponite	UV	1200	113
Sodium alginate	3–5%	Ionic	0.6–6.4	213
GelMA	3–5%	UV	75–2000	65
Hyaluronic acid	1.5%	Temperature	22	214
Collagen	1.5–1.75%	Temperature, pH	1.7–1.8	215

GelMA, gelatin methacryloyl; PEG-DA, poly(ethylene glycol) diacrylate; UV, ultraviolet.

in length, resulting in consistent mechanical properties.[81] Due to processes variations, natural polymers are typically more polydisperse than synthetic polymers.[82,83] Increasing polymer molecular weight, crosslink density, or concentration can improve the printability of the solutions at the cost of limited cell migration and a reduction in nutrient diffusion.[84] Polymer molecular weight, crosslinking mechanism, and side-groups dictate functionality of the polymer as a bioink and subsequent compatibility.[85] High molecular weight polymers are typically viscous due to an increase in chain entanglements.[86] Thus, many of these criteria can be used to gauge the overall bioprinting process and the interplay between material chemistry and mechanical stresses cells undergo during the printing process.

Rheology of bioinks

As extrusion-based bioinks must be injected through a printing gauge, the ability to flow is of utmost importance. Rheology is the study of flow properties of materials under external forces.[87] Unfortunately, rheology data presented often lacks the contextual relationship of the rheology to the printing results. Recent studies are beginning to understand the correlation that exists between the rheology of bioinks and the subsequent shape fidelity.[88] In this study, we present an understanding of the various rheological tests that are available, their ability to predict potential of a bioink for 3D bioprinting (Fig. 3b), and the parameters that are often lacking in current studies.

Rheological characteristics of bioinks are determined using either a stress or a strain-controlled rheometer. Rheometers either apply a specific displacement or force, both of which can either be applied in oscillation (back and forth) or in rotation (unidirectional). Various parameters such as storage modulus (G'), loss modulus (G''), and viscosity (η) are calculated and can be used to define the printability of bioink formulations.[87,89] Storage modulus is a measure of the elastic energy within the bioink, while loss modulus is a measure of the viscous portion or dissipated energy within the bioink.[39] Both storage and loss modulus are calculated while performing oscillatory measurements. Viscosity, calculated *via* rotational tests, measures the material's resistance to flow.[21]

Typically, bioink characteristics are determined using an oscillatory amplitude or frequency sweep to demonstrate the storage and loss modulus and a rotational shear-rate sweep is performed to determine viscosity.[67] Storage and loss moduli can be determined for precrosslinked or post-crosslinked bioinks as a measurement of bioink performance. Viscosity is used to describe the ability of the bioink to flow through the reservoir, needle, and onto the printing surface.[90] After extrusion, a bioink must quickly recover or be crosslinked so that it does not spread on the printing surface.[91] These rheological characteristics are crucial to define the printability of bioink and will be discussed in detail.

Viscosity. For extrusion-based bioprinting, a high viscosity at low shear rate is necessary to ensure that the bioink does not spread and prevent collapse of large structures. Viscosity can be controlled by polymer molecular weight, degree of branching, concentration, and addition of rheological modifiers.[68] Generally, an increase in these parameters results in an increase in viscosity across all shear rates. This is illustrated in Table 1, which details a list of commonly used polymers for bioinks. Conversely, lower crosslinking density within hydrogel matrix aids in cell proliferation, migration, and tissue formation through the facilitation of nutrient diffusion and waste removal.[92] Importantly, the viscosity of a hydrogel bioink can directly influence the resulting shape fidelity such as drooping and spreading.

Viscosity influences the ability of bioink to flow. An increase in surface tension between the needle gauge and bioink will decrease the ability of the bioink to shear thin, whereas an ideal, frictionless system will facilitate extrusion.[93] Overall, the bioink viscosity dictates whether extruded materials are droplets, a continuous filament or strand.[36] Low viscosity solutions of GelMA tend to form droplets that either will be forcefully expelled or form large droplets that gravity causes to separate from the nozzle.[94] However, rheological modifiers, such as nanosilicates[95–97] or hyaluronic acid,[94] can be added to GelMA to increase the viscosity and form a filament rather than a droplet. Filament formation allows for high-fidelity 3D structures to be formed rather than a puddle.

Shear-thinning ability. Shear rate sweeps are most commonly used to predict the behavior of a bioink during the printing process, determining viscosities across a range of shear rates. Shear rate sweeps often apply a range of shear rates, from low shear rate ($<10^{-3}$ s^{-1}) to high shear rates ($>10^{2}$ s^{-1}), to mimic the bioink going through a needle. For bioinks, a high viscosity at low shear rates and low viscosity

at high shear rates is imperative for the extrusion process.[98] Materials that exhibit this characteristic are called "shear-thinning."[8,65] Often characteristic shear rate versus viscosity graphs are presented with a lack of details.

Several models have been developed that can describe the ability of a hydrogel to shear thin. Classically, the power-law model, which is explained through the equation $\eta = K\gamma^{n-1}$, where η is viscosity, K is the flow consistency index, and n is the shear-thinning index, has been applied to materials where a low shear rate or high shear rate viscosity plateau is not observed. The power law index can describe the degree of shear-thinning. When $n = 1$, the solution is Newtonian; $n < 1$ shear thinning; and $n > 1$ shear thickening.[99] While graphical interpretation informs readers that materials are shear-thinning, equation fitting may bring broader understanding to the data collected and an overall conclusion regarding the ability of a bioink to be extruded through needles (Fig. 3c).

For example, the rheological profile of alginate precursors has been investigated using the Generalized Power-law equation.[50] Through the application and study of the flow consistency index, it was concluded that $n \sim 0.3$–0.4 has an appropriate flow profile for bioprinting applications. In addition, the yield stress was examined as a critical parameter that dictates cell viability during the printing process. Other work suggests that hydrogel precursor modulus is important for cell delivery.[100] Uncrosslinked bioink viscosity and storage modulus are analogous measurements, with the viscosity measuring resistance to flow, while storage modulus is an interpretation of hydrogel stability.

The use of shear-thinning information to predict the ability of a bioink to be 3D printed has also been investigated. We would like to make the important distinction of being able to inject materials versus 3D printed bioinks: 3D printing requires a bioink to stabilize or localize at a given point, while injection only requires materials to be shear-thinning. Once the bioink has exited the needle, there are little to no shear forces exerted on the bioink.[101] To achieve more accurate rheological predictions for 3D bioprinting applications, researchers are encouraged to calculate the shear rates experienced throughout the 3D printing process, program rheological tests to apply these specific shear-rates, and examine the viscosity recovery. In a recent study, a recovery time of 30 s was deemed appropriate and percentage recovery was measured as a comparison between unsheared and postsheared bioinks.[102]

Researchers often use hydrogel precursors during the extrusion process, utilizing viscosity as the de facto measurement of choice via a rheometric viewpoint. In addition, thixotropic loops (increasing shear rate followed by a decreasing shear rate in a set amount of time) describe the internal structure rebuilding time.[103,104] A perfectly Newtonian bioink will have overlapping curves for both the increasing and decreasing shear rates, indicating the presence of a minimal internal structure and a nonideal bioink candidate.[104] A difference between loading and unloading curves indicates the degree of thixotropic behavior within the context of the test (i.e., if the test was completed using a 1 min loading and 1 min unloading curve, thixotropy is specific to the time frame applied).[105] Thixotropic loop tests can be difficult to interpret and often require specialized "cup and cone" geometries to obtain reliable results.

Yield stress. Bioinks must overcome a certain amount of stress, deemed yield stress, to allow for flow from the barrel and onto the printing bed. Yield stress is the minimum stress that must be placed on the material for flow to occur. Hydrogel precursors are typically a weak network. When a stress is applied above the yield stress, these network interactions are interrupted, permitting the material to flow.[106,107] For example, gelatin is a thermoresponsive hydrogel, and above $\sim 37°C$, it has high chain motility due to weak polymer–polymer interactions and can easily be extruded through a needle when stress is applied. High yield stresses pose process difficulties in cell incorporation and in the work required for the 3D printer motor. Along with gelatin, other hydrogels, such as a self-assembling peptide[108,109] and colloidal systems,[110,111] have been developed that incorporate lower yield stress as an important design consideration.

Oscillatory thixotropic measurements further elucidate bioink stability during printing process. To complete oscillatory thixotropy measurement, an amplitude sweep must first be conducted to determine the linear viscoelastic regime of a bioink. Specifically, the storage modulus and loss modulus should be independent of the applied stress or strain (both of which are amplitude modulated). Outside of the linear regime, the bioink is dependent on higher order harmonics, requiring more advanced knowledge for data interpretation. A yield point, where the storage modulus decreases below the loss modulus ($G' < G''$) is exhibited, is typically demonstrated at amplitudes above 10^1 Pa or between 50% and 1000% strain.[112]

Oscillatory thixotropic tests, apply series of sequential amplitudes, simulating printing conditions. First, an amplitude below the yield point is applied, representing $G' > G''$. This is followed by application of a higher amplitude ($G'' > G'$), which represents the flow through the needle. The last step is application of the original amplitude, with the expectation that G' will increase quickly back to the original value.[113] Traditionally, researchers have tested multiple cycles, although the 3D printing process requires only one application of a high amplitude since the bioink must only traverse the length of the needle once.

Print fidelity

Bioink composition is extremely crucial in designing prints with high resolution and fidelity. High viscosities at low shear rates dictate construct fidelity. Often, bioinks lack recoverability, resulting in printed structures with lower resolutions and accuracies than can be achieved with other additive manufacturing techniques. However, when shear-thinning behavior, yield stress, and recoverability are examined holistically, high fidelity prints can be achieved. Achieving a synergistic balance between shear-thinning, yield stress, and shear recoverability is required as the complexity of printing increases from one-dimensional (1D) to 3D (Fig. 3d).[114] Another important parameter which governs fidelity of constructs is the swelling behavior of the hydrogel ink, which is mainly determined by the charge densities and extent of crosslinking.[94,115] High crosslinking densities support lower swelling ratios and provide high fidelity prints but reduce oxygen and nutrients diffusion, thereby reducing cell viability in the constructs. A solution

to this problem is to design a composite bioink combining hydrogel materials, which provide enhanced cell activity with a material that confers mechanical stability, thus arriving at good print fidelity.[116]

Postprinting Considerations and Assessment

Upon establishing cytocompatibility, the bioink can be printed into complex shapes and geometries. However, there are additional biological and mechanical characteristics that need to be taken into consideration postprinting.

Physiological stability of 3D bioprinted structures

Structural fidelity. Rheology is an important tool to determine the potential of a bioink for printing, specifically characterizing the ability of the bioink to deform and recover. However, after printing, image analysis of extruded bioinks provides additional information concerning spreading of bioinks (Fig. 4a). Several methods have been used to analyze the quality of extrudate. The 3D printing process begins in designing a construct in a CAD program (i.e., AutoCAD or SolidWorks).[117] Given the programmed design and dimensions, the print fidelity can be characterized by comparing the experimental, extruded dimensions to the theoretical ones. Light microscopy or micro-computed tomography has been used to image printed constructs.[113,118] Ouyang *et al.* devised a system of images and equations to quantify the ''printability'' of extruded bioinks.[89] Three classes of printability were established (under gelation, proper

gelation, and over gelation) to describe the morphology of the extruded samples. Proper gelation bioinks exhibited smooth surfaces with regular grid patterns; under gelation bioinks flowed together creating circle patterns rather than squares; over gelation bioinks had irregular grid patterns.

Mathematically, printability (Pr) was defined as $Pr = \frac{\pi}{4} \frac{1}{C} = \frac{L^2}{16A}$, where C is the circularity of the print, L is the length, and A is the area. Pr values <1 indicate poor fidelity with spreading and large, curved corners. As Pr approaches 1, the print ''exactly matches and corresponds to the model design,'' with precise angles, smooth prints, and exact deposition of material. As Pr increases, the bioink became jammed or ''crinkly''/rough (ridges formed, cracks were prominent, and the overall print was poorly constructed). Mathematically defining print fidelity is an important milestone within the bioprinting literature. However, printability is defined in only 1D or two-dimensional (2D), and there is a need to develop new approaches to evaluate 3D printability.

Mechanical stability and elasticity. Native tissue moduli are well characterized. Therefore, composing a material to match should, in essence, provide mechanical stability of the implanted hydrogel.[119–121] Elastic moduli characterization is a classic method to study the ability of bioink to withstand deformation. Elastic moduli can be determined from the slope of a stress versus strain curve in compression or tension (Fig. 4b). However, there are discrepancies or limitations between the parameters defined within each test (i.e.,
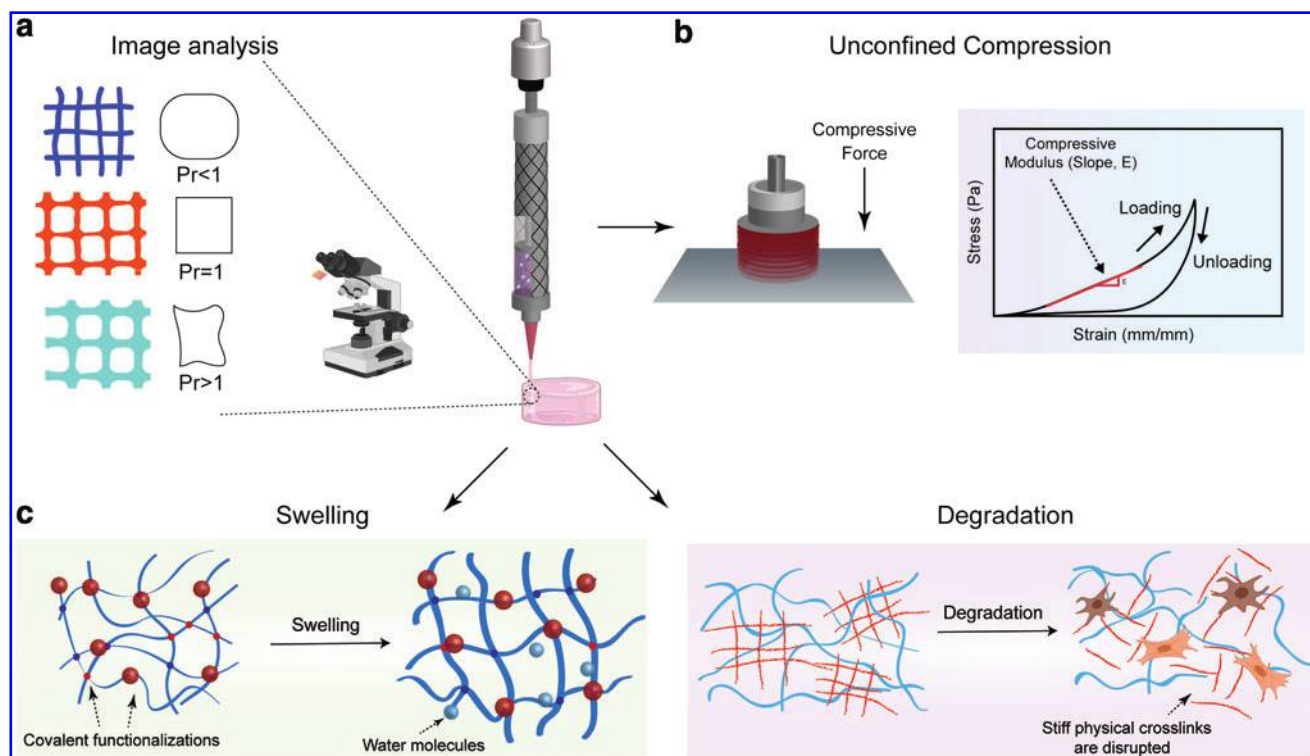

FIG. 4. Postprinting considerations. **(a)** Optical image analysis is performed to examine the quality, spreading and printability of the bioinks postcrosslinking. **(b)** Compressive mechanical analysis is performed to evaluate the mechanical stability and compressive modulus of the 3D bioprinted construct. **(c)** Swelling and degradation analysis aids in determining swelling ratio and degradation characteristics of the bioink, which is crucial in designing 3D bioprinted elements for specific tissue engineering applications. Color images are available online.

compression/tension). For example, when defining the ultimate tensile/compression stress, the range of strain over which testing is performed is limited. Specifically, a material can only be compressed ∼90–99%, while under tension the construct can be theoretically stretched indefinitely.

The bioprinting process deposits bioink layers that must adhere to each other to form a mechanically rigid structure. The potential for delamination of layers due to low adhesion results in a defect, thus increasing the chance for stress concentrators and crack propagation.[122,123] Mechanical compression/tension testing can be performed to evaluate the mechanical properties of 3D printed structures compared to bulk properties. Compression testing of cast bioinks en-

sures that the structure does not have void spaces within the tested samples (assuming no bubbles, sufficient layer contact, and clean removal from the printing bed). Casted bioinks typically have low polymer alignment since the material is allowed to conform to the surrounding mold. However, due to the layer-by-layer material deposition in the 3D printing process, void spaces can develop or the polymer may align, ultimately producing a significantly different mechanical profile. Ideally, the printed sample should possess 100% layer adhesion and contact. However, when using a circular gauged needle, there might be some space due to a geometric mismatch. From these spaces, cracks propagate and decrease the compressive modulus.[124]
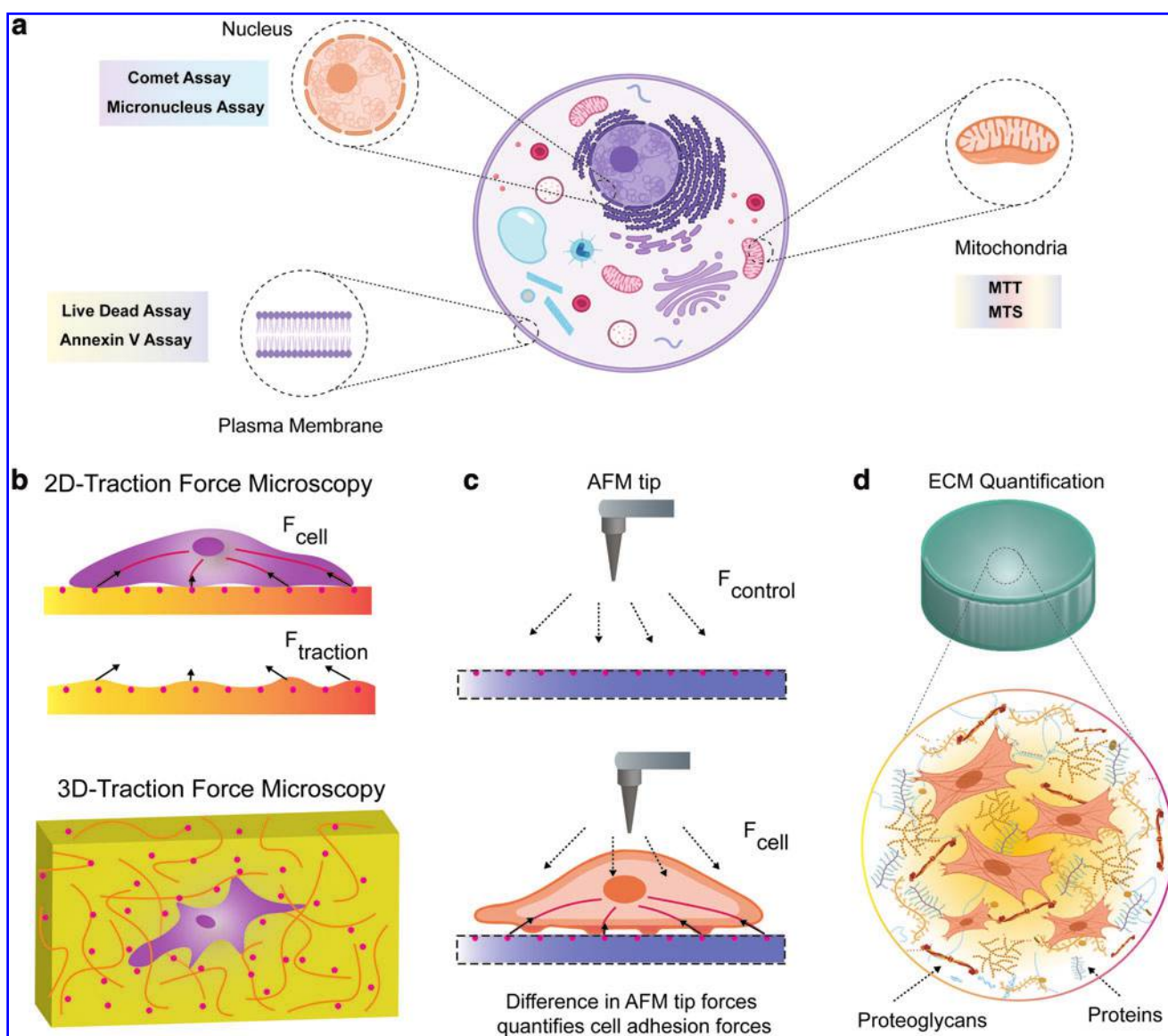

FIG. 5. Analyzing cell–material interactions. **(a)** Summary of various cellular cytotoxicity assays to monitor cellular viability post 3D bioprinting. **(b)** Traction force microscopy analysis is used to determine the traction force cells generate when attached to the bioink. **(c)** AFM techniques also quantify cell adherence to bioink through AFM cantilever deflections. **(d)** Extracellular matrix quantification through various colorimetric assays determine how cells operate once encapsulated in the bioink, which is crucial as the 3D bioprinted scaffold simulates the native tissue 3D architecture. AFM, atomic force microscopy; MTS, 3-(4,5-dimethylthiazol-2-yl)-5-(3-carboxymethoxyphenyl)-2-(4-sulfophenyl)-2H-tetrazolium; MTT, 3-(4,5-dimethylthiazol-2-yl)-2,5-diphenyl tetrazolium bromide. Color images are available online.

Swelling and degradation. Once the bioink is cross-linked and placed into either an implanted site or in cell culture media, swelling of the structure occurs. Swelling can influence postprinting mechanics: an increase in fluid increases the distance between crosslink or net points and decreases crosslink density.[125] Swelling can also be beneficial, as it allows for diffusion of any entrapped therapeutics and cellular waste products.[126] Bioinks composed of natural polymers such as gelatin will both swell and degrade due to enzymes secreted by cells. Gelatin-based hydrogels have previously been used for bioinks, demonstrating a mass loss of 65% within 11 h when submerged in a collagenase solution (5 U/mL).[127]

Synthetic bioinks must be designed to degrade within an appropriate time-scale for the intended application. Poly(lactide-co-glycolide) compositions are often used to regulate the degradation profile of hydrogels or nanoparticles[128,129] and for drug delivery applications.[130,131] Specifically, therapeutic release profiles can be modulated via encapsulation into PLGA nanoparticles with varying amounts of lactide and glycolide to allow for appropriate release times.[131] Alternatively, PEG has been modified with poly(lactic acid) end groups to modulate network degradation[132,133] and cell adhesion[134] and proliferation.[135] To fully recapitulate native tissue, degradation profiles are a key feature of developed bioinks that must be characterized further. Hence, swelling and degradation characterization of bioprinted constructs become crucial for understanding their behavior *in vivo* (Fig. 4c).

Effect of the printing process on cell viability

Estimation of cellular compatibility is an essential part to understand bioink–cell interactions and how the cells can be stimulated by the bioink. It is also important to evaluate the effect of shear forces and degradation byproducts on the bioprinted system. This is done through various cellular cytotoxicity/viability assays (Fig. 5a). The use of nanoparticles as rheological modifiers to bioink systems also creates challenges in terms of cellular toxicity. Unlike polymeric components of bioinks, whose behavior when interacting with cells is well documented, nanoparticles can interact with cells in a variety of methods, such as interaction with cytosolic proteins, effects on mitochondrial activity, and generation of reactive oxygen species.

Hence, it is paramount to identify concentration-dependent effects the nanoparticles have on the cells before use in printing applications.[136] These factors are also important for understanding the effects of polymer crosslinking agents on overall cellular viability.[137] A list of common assays used to determine cellular viability within printed constructs is in Table 2. However, a major drawback of these assays is the focus only on the cell viability and the lack of consideration

TABLE 2. LIST OF COMMON ASSAYS TO MEASURE CELL VIABILITY

Reagent	Site of action	Method of detection	Reference
Trypan blue	Cytoplasm	Trypan blue is excluded by live cells with intact plasma membranes, while dead cells are stained blue	216
LDH	Extracellular space	Release of LDH cytosolic enzyme into extracellular space. The released LDH is then measured via a tetrazolium dye.	217–219
TBARS	Cytoplasm	Estimation of lipid peroxidation due to ROS generation by quantification of Malondialdehyde present in cells.	220,221
Calcein-AM and ethidium bromide (Live/Dead assay)	Cytoplasm	Fluorescent probes commonly used together in the form of Live/Dead viability assay. Live cells are able to exclude Ethidium bromide, while dead cells do not show fluorescence for calcein.	222,223
Annexin V	Cell membrane	Early apoptosis detection, due to movement into the outer membrane of the plasma membrane	224
H_2DFCA	Cytoplasm	The cell-permeant H_2DCFDA is reduced to its fluorescent form inside cells in the presence of ROS.	225,226
Comet assay	Nucleus	DNA fragmentation is viewed by single cell gel electrophoresis.	227,228
Micronucleus assay	Nucleus	Study of DNA damage at the chromosome level. By differential staining of DNA and RNA through stains such as acridine orange, DNA with a micronucleus can be visualized. An increase in the frequency of micronuclei correlates to increased chromosomal damage.	229,230
MTT/MTS/WST	Cytoplasm/ mitochondria	Tetrazolium dye is reduced to insoluble purple colored formazan by oxidoreductase in living cells. Assuming the similar cell types and cell numbers, the dyes can be used as a colorimetric assay for determining cell metabolic activity.	231,232
JC-1 assay	Mitochondria	Aggregation of the dye is dependent on mitochondrial membrane potential. Upon aggregation, a shift in fluorescence occurs. This change in florescence can be used to determine mitochondrial membrane integrity.	233–235

H_2DCFDA, 2′,7′-dichlorodihydrofluorescein diacetate; LDH, lactate dehydrogenase; MTS, 3-(4,5-dimethylthiazol-2-yl)-2,5-diphenyl tetrazolium bromide; MTT, 3-(4,5-dimethylthiazol-2-yl)-5-(3-carboxymethoxyphenyl)-2-(4-sulfophenyl)-2H-tetrazolium; ROS, reactive oxygen species; TBARS, thiobarbituric acid reactive substance; WST, water-soluble tetrazolium salt.

of other processes such as cell differentiation, formation of cell signaling molecules, or secretion of proteins.[138] Advanced genetic testing, such as RNA-sequencing, may also be used to identify the effect of bioink components on cells, but this process is both expensive and time-consuming.[139]

During 3D bioprinting, encapsulated cells experience shear forces during the bioprinting process, which can affect cellular viability, adhesion, and proliferation.[50,100] Cell suspensions in high viscosity bioinks have been used to increase cell viability.[100] Along with viscosity, geometric constraints of the printing apparatus, such as the needle gauge shape and size, can influence the shear stress being applied to the material: large orifice deposition needles (small gauge number) reduce the shear stress, while simultaneously reducing resolution of the 3D print, and lower volumetric flow rates decrease the shear stress.[140] Shear stress has profound effects on cell phenotype and functionality. For example, at 1 Pa of shear stress, articular chondrocytes can significantly change morphology and metabolic activity,[141] whereas human mesenchymal stem cells (hMSCs) can withstand shear stresses in the range of 1×10^{-5}–1×10^{-4} Pa before significantly upregulating messenger RNA expressions of osteocalcin, Runx2, and alkaline phosphataste.[142]

In conjunction with the flow behavior of the bioink, internal shear stress can influence cell viability. Mechanotransduction at the cell-material interface and the mechanical stress placed on cells within the bioink continue to be hurdles for 3D bioprinting constructs. Current techniques to study cell viability as a function of shear stress rely on 2D culture and varying the flow rate of media above the cells. Short term, high shear stress, with cells suspended in a moving medium is less studied, although cells appear to be resilient to the printing process.[143,144] Bioinks such as GelMA,[94,145] alginate,[50,146] and PEG[147,148] along with materials such as, peptides,[149–151] polycaprolactone,[152–154] kappa-carrageenan,[57,155] and others[156–158] have been extensively explored to comprehend the interplay between printing parameters and cellular response to the bioprinting process.

GelMA-based scaffolds were used to 3D print complex shapes[145] and were used to deposit HepG2 cells with favorable viability.[143] Alginate is often used due to its non-immunogenicity, ability to shear thin, and quick ionic crosslinking in $CaCl_2$ solutions.[159] The effects of bioink compositions (0.5–1.5 wt./vol. %) and printing pressures (0.5–1.5 bar) on cell viability have been investigated.[50] hMSCs were >60% viable at shear stress >10 kPa, nearing 100% viability with shear stress <5 kPa. In a similar recent work, PEG-based bioinks were developed with human dermal fibroblasts. It was found that before a critical flow rate of ~ 140 mg/s bioinks with a lower mass flow rate exhibited a linear relationship with cell viability and with decrease in mass flow rate, cell viability decreased. This indicated that increase in hydrogel robustness led to a proportional damage on encapsulated cells.[160] Thus, it is crucial to determine the shear rate distribution within the bioink formulations.

Evaluating cell–material interactions

Concurrent with the cellular viability, cell functions such as adhesion, proliferation, and/or differentiation should also be monitored. Cells encapsulated within the bioink can proliferate and deposit nascent ECM that is composed of a complex network of proteins (collagen, elastin, laminin, and fibronectin), glycoproteins, and proteoglycans.[161] This newly deposited ECM can provide structural and biochemical support to encapsulated cells.

The mechanical stiffness and elasticity of the ECM varies from one tissue type to the next, primarily due to changes in the ECM compositions (in particular elastin and collagen), and the stiffness can differ by several orders of magnitudes. For example, the elastic modulus of soft brain tissue is in the range of tenths of a kilopascal (kPa), while calcified bone is in the range of megapascals (MPa).[162] The change in ECM composition in diseased tissue, particular in case of cancer metastasis, is well documented.[163–166] The ECM protein collagen also plays an important role in cellular adhesion. The process of cell adhesion onto the ECM is a complex biochemical process that has to be lined with other cellular events such as cell differentiation, cell migration, and the cell cycle.[167]

Both ECM cell adhesion sites and mechanical properties are of paramount importance when selecting biomaterial constituents. The main goal of a fabricated ECM is to provide adequate sites to the cell for binding, as well as a 3D architecture and mechanical stiffness similar to the native tissue. Careful bioink selection allows for the generation of a 3D architecture that faithfully mimics the native tissue, while allowing for the variation in the overall mechanical stiffness and the chemical properties by changing the bioink composition or concentration.[168]

Most commonly, cell–material interactions are commonly measured via 2D seeding of cells on the bioink surface. While useful, these techniques fail to fully capture the complex interactions when cells are encapsulated with 3D matrices. The 3D encapsulation of cells within hydrogels represents an increasingly complex technique for cell culture, but permits for the fabrication of constructs that further recapitulate the innate cellular architecture of tissue scaffolds for engineering applications.[124] This 3D microenvironment better mimics what cells experience *in vivo*, compared to standard tissue culture. In designing new bioinks for extrusion bioprinting, initial cell screenings continue to be an established method to determine cell–material interactions. Thus, it is important to evaluate cell–matrix interactions as well as deposition of nascent ECM protein using various available techniques.

Cell–matrix interactions within 3D printed structures. Traction force microscopy (TFM) is used to determine the traction force between cells and materials. Using the traditional TFM techniques, cells are cultured on a clear polyacrylamide gels that are functionalized with adhesive ligands and contain fluorescent beads that are embedded just below the gel surface.[169] When attachment occurs, cells generate a traction force that moves the fluorescent beads. This movement is then quantified by measuring the displacement of the fluorescent bead (Fig. 5b). This technique has been used to compare cellular forces generated by metastatic breast, prostate, and lung cancer cell lines and their nonmetastatic cell line analogs. The traction forces of the metastatic cell lines were found to be higher.[170] After seeding cells, TFM could be used to determine where cells are adhering on the bioinks surface and subsequently moving. However, this requires an optically transparent bioink as well as a flat surface to image. Alternatively, vinculin staining can be used to monitor focal adhesion points and elucidate cell binding.[171]

3D TFM is a modification to TFM and does not require that cells be on the exterior of the sample being analyzed. 3D TFM can be used to understand cell behavior in 3D cultures (Fig. 5b). In 3D TFM, fluorescent beads are coencapsulated with the cells within the bioink. A limitation of this technique is the modification of the bioink's rheological properties due to the addition of fluorescent beads. However, this method can provide valuable insight on cell behavior within a bioink. Fraley *et al.*[172] used these techniques to track the movement of focal adhesion proteins in the 3D matrix and establish their role in cell motility. Transparent samples are preferred due to the ability to clearly visualize the fluorescent beads.

Atomic force microscopy (AFM) probe techniques involve the quantification of how strongly a cell is adhered to the surface of the bioink. The AFM cantilever reaches the cells from micrometers above slowly. The cantilever then makes contact and indents it such that the deflection reaches a set point. The cantilever deflections during this process are recorded as force–distance curves, where the highest force is the cells adhesion strength (Fig. 5c). This technique can be used to measure both cell–cell adhesion forces and cell–matrix adhesion forces.[173] While using AFM with bioink systems, the cells in the printed constructs must come in contact with AFM tip. Fully encapsulated cells cannot be sensed utilizing AFM techniques without destruction of the printed construct.[174]

Multiple particle tracking microrheology (MPT) is another technique used to quantify cell–matrix interaction. In this technique, probe particles are embedded in the hydrogel matrix. The Brownian motion of the embedded particles is measured and related to rheological properties such as creep compliance and viscosity.[175,176] PEG-based peptide cross-linked hydrogel scaffolds were seeded with hMSCs. MPT data were gathered over a period of time, which aided characterization of spatial remodeling of the hydrogels as the hMSCs migrated.[177] MPT is a crucial technique, which identifies regions in the hydrogel network where cells adhere during matrix degradation and MMP secretion. It also characterizes distances over which cellular matrix remodeling occurs.

Evaluating nascent extracellular matrix production within printed structure. Along with the visualizing cell interactions with bioinks, evaluation of deposited matrix and protein quantification enhances the understanding of how cells are behaving. The production and deposition of ECM by cells is an important cellular event. In the case of bioprinting, it becomes essential for cells to produce ECM to facilitate further proliferation within the scaffold. Native ECM is composed of various components, such as proteins (collagen, elastin, and fibronectin) and glycosaminoglycans (GAGs) (heparan sulfate, chondroitin sulfate, and so on).[178] Hence, it is important to quantify the production of ECM components in 3D printed scaffolds (Fig. 5d), as they could mimic the 3D architecture of the native tissues. Various methods can be used for determining the individual components as listed below.

Collagen is the most abundant protein within the human body and is an important ECM component. The most common methods to estimate collagen production is the quantification of hydroxyproline within a sample. This is done by dissolving the sample in hydrochloric acid, followed by neutralization, and further reaction with reagents such as chloramine T.[179] This method has a distinct drawback of being rather tedious and can greatly be affected by the type of sample. Hence, simpler colorimetric methods have been developed using dyes such as Sirius Red F3BA, which bind specifically to collagen and show no specific binding with elastins.[180]

There are five types of GAGs: heparan sulfate (HS), chondroitin sulfate, dermatan sulfate, keratan sulfate, and hyaluronan, of which HS is the most studied.[178] There are two commonly used techniques for the quantification of GAGs, namely Alcian Blue and Dimethylmethylene Blue (DMMB) assay. The latter works on the principle of acid digestion of the polysaccharide followed by reaction with a carbazole, which gives rise to a colored byproduct.[181] However, this method has a tendency to overestimate the concentration of the GAGs due to interference from pH buffer components, such as chloride ions (present in phosphate-buffered saline).[182] The DMMB assay relies on the ability of sulfated GAGs to bind the cationic dye 1,9-dimethylmethylene blue[183] and, hence, is better suited for GAG quantification.

With both collagen and GAG quantification, standardization to the number of incorporated cells provides information regarding how active the cells are and if they are proliferating. Nascent protein deposition within the 3D printed construct can be visualized by adapting a recently developed labeling technique. In this technique, methionine molecules containing azide groups are incorporated into proteins during their synthesis. These labeled proteins are then visualized for a spatiotemporal characterization of nascent protein deposition across the hydrogel matrix environment.[184,185]

Future Directions

The field of 3D bioprinting has undergone rapid progress over the last several years. There has been headway in optimizing bioinks which not only provide cell viability and printability but also provide additional tunable functionalities, such as stimuli responsiveness and programmable properties. There has also been progress in expanding the hardware of 3D bioprinting to incorporate synergistic, multimaterial printing. In the following sections, we will examine the various emerging bioprinting techniques and their attributes which make them attractive in this field.

Multimaterial 3D bioprinting for fabricating complex architectures

Current printing modalities successfully print relatively complex geometries but are not completely successful at recapitulating the intricate compositions of native tissue structures. Progress in various additive manufacturing techniques has led to the development of multimaterial bioprinting.[186–191] Multimaterial extrusion printing enables for the deposition of multiple bioinks in a coded, continuous manner to fabricate tissue constructs with a smooth and fast transition between different materials (Fig. 6a). This enables for printing structures that closely mimic native tissue designs and composition.[192]

The multiextrusion process is calibrated with the motorized stage movement, allowing for deposition of 3D architectures with multiple bioinks in a spatially defined manner. However, resolution and print fidelity still remain significant challenges, which are being met by designing additive
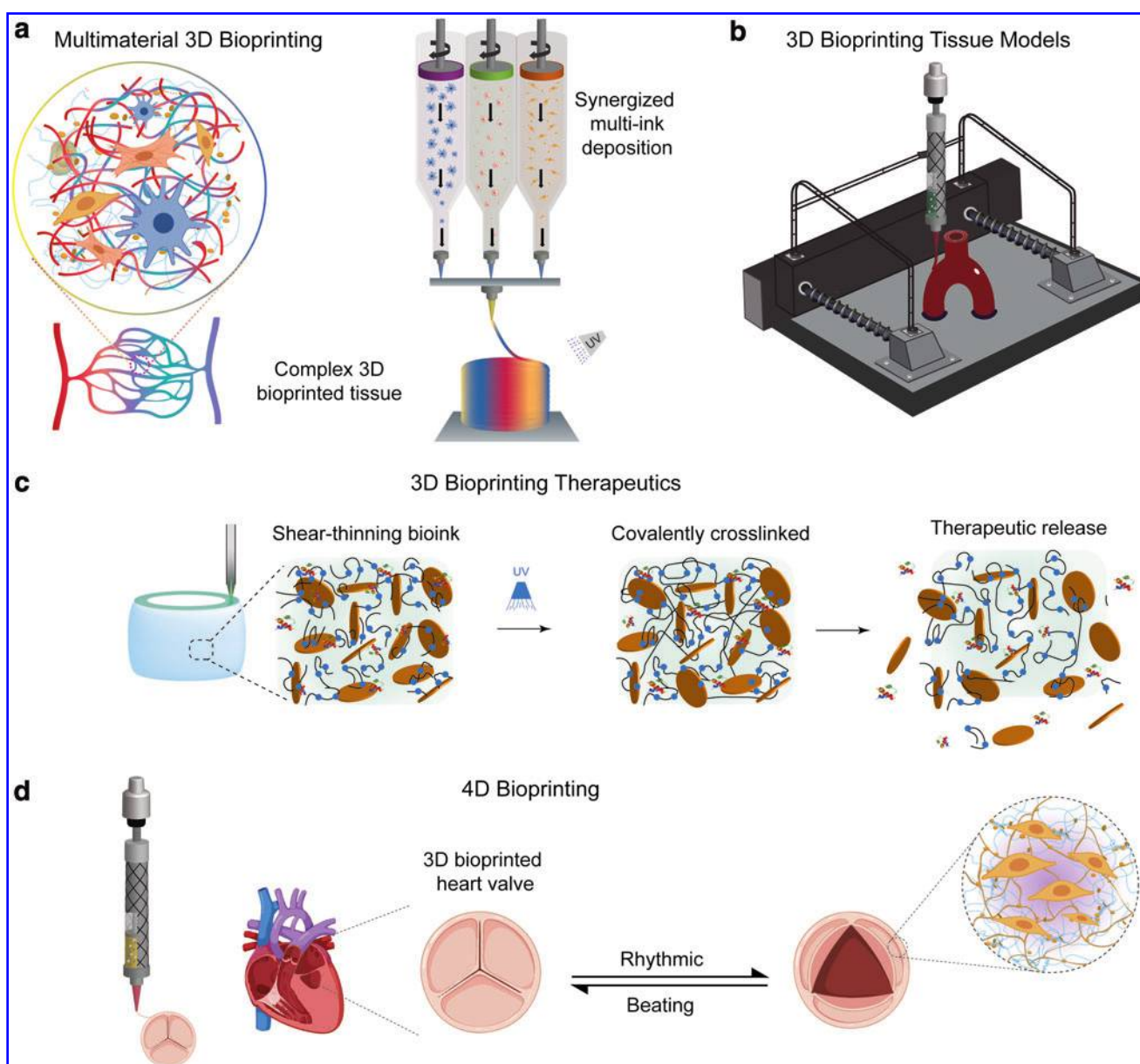
FIG. 6. Future directions. **(a)** Multimaterial 3D bioprinting aims to recapitulate intricate composition of native tissue structures through printing multiple bioinks in a synergistic manner. **(b)** 3D bioprinting engineered tissue models enables conceiving *in-vitro* biomimetic tissue models which can be utilized in understanding disease progression and treatments for conditions such as cancer. **(c)** 3D bioprinting therapeutics utilizes bioinks engineered with protein therapeutics which can direct cell function in the bioprinted construct. **(d)** Four-dimensional (4D) bioprinting supports designing programmable structures with tunable behavior and functionalities. A bioprinted heart valve tissue is responsive to electrical impulses generated by cardiac cells and exhibits rhythmic contraction and expansion. Color images are available online.

manufacturing systems that can precisely control the printing of complex architectures.[50] Theoretical modeling is also being applied to the bioink design. Instructing the experimental design of a tissue structure through modeling is expected to enhance the function and properties of biofabricated tissue structures.[193]

3D bioprinting tissue models for preclinical evaluation

Engineered tissue models are becoming an increasingly appealing platform to study various diseases and predict the efficacy of novel therapeutic interventions, potentially re-

ducing or eliminating animal subjects.[194] However, traditional fabrication techniques tend to produce oversimplified constructs and cell microenvironments.[195] The advent of 3D bioprinting allows for engineering of complex, biomimetic *in vitro* tissue models that can aid in treatment optimization.[196] For example, the tumor microenvironment is considered extremely vital in understanding and regulating tumor metastasis and progression.[197] 3D bioprinted tumor models enable a more precise simulation of the tumor environment and are ideal for preclinical studies (Fig. 6b). A 3D printed coculture ovarian cancer model was 3D printed in a controlled manner using normal fibroblasts and human

ovarian cancer cells (OVCAR-5). It was observed that the 3D printed cancer model established 3D acini with growth kinetics and structures similar to *in vivo* development.[198] Despite progress in designing cancer models through 3D bioprinting, there still is a limited scope of engineering models with multicellular microenvironments consisting of cancer cells, immune cells, noncancer cells, and vascular cells.

Printing therapeutics in 3D to control and direct cellular functions

Progress has also been made in designing bioinks loaded with therapeutics, which can be utilized to program cell function within printed constructs. For example, a bioink designed from a hydrolytically degradable polymer poly(ethylene glycol)-dithiothreitol (PEGDTT) and 2D nanosilicates loaded with protein therapeutics demonstrated a shear-thinning rheological profile with enhanced printing fidelity.[199,200] The anisotropic charge of the 2D nanosilicates enables sequestering of protein therapeutics and facilitates their sustained release within the 3D printed structure (Fig. 6c). This approach exhibits the potential to engineer intricate 3D tissue structures within regenerative medicine.

4D bioprinting for designing dynamic tissues

The process of four-dimensional (4D) bioprinting involves 3D bioprinting structures that change upon exposure to an external stimulus, such as light, heat, or moisture. These triggers allow the constructs to change shape, functionality, or properties with the potential to translate into dynamic motion.[201] With detailed insight on material properties and their stimuli responsive behavior, 4D bioprinting allows for the design of programmable structures with tunable functionalities. Examples of materials used for 4D bioprinting include shape memory polymers (SMPs)[202,203] and hydrogels.[204,205] 4D printing with SMP-based inks involves embedding SMP fibers within a matrix to constitute a 3D bilayer structure. A dynamic shape transformation of these structures can be achieved by heating the construct above the characteristic transition temperature exhibited by the SMP.[206] Heat-activated SMPs have been used in making 4D printed smart stents, which are deformed to transitory shape, introduced into the body and then transformed back to the original shape with a localized temperature change.[202]

In the case of hydrogel-based bioinks, 4D bioprinted composites with a bilayer framework exhibit controlled deformations that depend on the hydrogel's swelling ratios, elastic moduli, and thickness of the framework.[201] Using modeling techniques allows for precise prediction of geometric changes of the configurations and generated movements, enabling design of constructs capable of twisting, folding, and/or curling. These hydrogel bioinks can potentially be utilized to bioprint various functional tissue components, such as printed functioning cardiac tissue[207] or personalized replacement heart valves (Fig. 6d).

Recently, semisynthetic approaches have been developed to enable photomediated 4D site-specific protein patterning. In these techniques, diverse library of homogeneous functionalized proteins were developed with reactive handles for biomaterial modification.[208,209] Mask-based photolithography techniques were utilized to control the protein patterning throughout hydrogel thickness. The photoreversible immobilization of proteins can be extended to growth factors and enzymes enabling a dynamic spatiotemporal regulation of cellular proliferation and protein kinase signaling. These techniques can be utilized to design advanced photoresponsive bioinks for 4D bioprinting.

Conclusion and Outlook

3D bioprinting is a multifaceted fabrication technique for printing complex tissue or even organ structures. The field of bioprinting is rapidly evolving with applications in engineering, science, and regenerative medicine. There has been significant progress in designing intricate biomimetic constructs with cellular functionalities. In general, bioprinting has emerged as a strong high-throughput platform technology to conceive macro- and microscale bioengineered systems. Although current techniques to assess polymeric bioink functionalities for 3D bioprinting applications are widespread, there is little standardization within the field. In addition, there remains an overall lack of bioink formulations and methodology for predicting usefulness as a bioink.

Clinical application of extrusion-based bioprinting requires bioinks that can be organized to replicate tissue organization, support cell proliferation and differentiation, and degrade at physiological time scales. The rheological properties of bioinks correlate to the systems biological performance, dictating the need for novel and precise analysis techniques to monitor cell/material interactions during the printing process. Optimization of the rheological properties, specifically yield stress, may permit homogeneous cell incorporation and further boost the printing process. Often high resolution is sought in 3D bioprinting, although recent studies suggest that high precision may not be necessary.[210,211] Thus, development of advanced bioink materials and formulations with suitability for multiple cell and tissue types is currently an area of focus.

Overall, there is a need to promote fundamental rheological understanding with utilization of biological techniques specifically to further deepen our insight into extrusion-based 3D bioprinting. In addition, there is a need to develop computational techniques that consider the bioink properties and mechanics during fabrication, such as nozzle diameter or printing speed, to provide a holistic approach to 3D bioprinting. Concurrently, there is a strong sense in the bioprinting community to make the printing modalities more accessible. We also need to bring down the cost of bioprinters and making them more available to a broader scientific group.

In the near future, we anticipate development of hybrid bioprinting systems capable of dispensing multiple biomaterials, multiple cell populations, as well as multiple biochemical cues (such as drugs, nutrients, and growth factors) bringing us one step closer to whole tissue/organ regeneration. These would also lead to advancement of biomanufacturing technologies with *in vivo* integration, leading to engineering constructs with enhanced *in-vivo* efficacy. Furthermore, stimuli responsive bioprinting strategies are also set to transform health care and medicine by development of dynamic constructs poised to be utilized in biosensing, bioactuation and biorobotics. Thus, this review

attempts to elucidate the 3D bioprinting process, detailing its various attributes. It also attempts to provide a deeper understanding of the mechanics governing bioinks and their subsequent macroscopic properties, such as ability to modulate adhesion, degradation, and therapeutic delivery for executing prints with higher resolution, fidelity, and biocompatibility.

References

1. Gibson, I., Rosen, D.W., and Stucker, B. Design for additive manufacturing. In: Additive Manufacturing Technologies. Boston: Springer, 2010, pp. 299.
2. Skardal, A., and Atala, A. Biomaterials for Integration with 3-D Bioprinting. Ann Biomed Eng **43,** 730, 2015.
3. Sorkio, A., Koch, L., Koivusalo, L., et al. Human stem cell based corneal tissue mimicking structures using laser-assisted 3D bioprinting and functional bioinks. Biomaterials **171,** 57, 2018.
4. Keriquel, V., Oliveira, H., Rémy, M., et al. In situ printing of mesenchymal stromal cells, by laser-assisted bioprinting, for in vivo bone regeneration applications. Sci Rep **7,** 1778, 2017.
5. Solis, L.H., Ayala, Y., Portillo, S., Varela-Ramirez, A., Aguilera, R., and Boland, T. Thermal inkjet bioprinting triggers the activation of the VEGF pathway in human microvascular endothelial cells in vitro. Biofabrication **11,** 045005, 2019.
6. Nakamura, M., Kobayashi, A., Takagi, F., et al. Biocompatible inkjet printing technique for designed seeding of individual living cells. Tissue Eng **11,** 1658, 2005.
7. Chimene, D., Peak, C.W., Gentry, J.L., et al. Nanoengineered ionic–covalent entanglement (NICE) bioinks for 3D bioprinting. ACS Appl Mater Interfaces **10,** 9957, 2018.
8. Wilson, S.A., Cross, L.M., Peak, C.W., and Gaharwar, A.K. Shear-thinning and thermo-reversible nanoengineered inks for 3D bioprinting. ACS Appl Mater Interfaces **9,** 43449, 2017.
9. Elisseeff, J., Anseth, K., Sims, D., et al. Transdermal Photopolymerization of poly (ethylene oxide)-based injectable hydrogels for tissue-engineered cartilage. Plast Reconstr Surg **104,** 1014, 1999.

10. Tan, H., and Marra, K.G. Injectable, biodegradable hydrogels for tissue engineering applications. Materials **3,** 1746, 2010.
11. Tharp, K.M., Jha, A.K., Kraiczy, J., et al. Matrix-assisted transplantation of functional beige adipose tissue. Diabetes **64,** 3713, 2015.
12. Kang, H.W., Lee, S.J., Ko, I.K., Kengla, C., Yoo, J.J., and Atala, A. A 3D bioprinting system to produce human-scale tissue constructs with structural integrity. Nat Biotechnol **34,** 312, 2016.
13. Hern, D.L., and Hubbell, J.A. Incorporation of adhesion peptides into nonadhesive hydrogels useful for tissue resurfacing. J Biomed Mater Res **39,** 266, 1998.
14. Zhou, M., Smith, A.M., Das, A.K., et al. Self-assembled peptide-based hydrogels as scaffolds for anchorage-dependent cells. Biomaterials **30,** 2523, 2009.
15. Brandl, F., Sommer, F., and Goepferich, A. Rational design of hydrogels for tissue engineering: impact of physical factors on cell behavior. Biomaterials **28,** 134, 2007.
16. Ventre, M., Causa, F., and Netti, P.A. Determinants of cell–material crosstalk at the interface: towards engineering of cell instructive materials. J R Soc Interface **9,** 2017, 2012.
17. Kisiday, J., Jin, M., Kurz, B., et al. Self-assembling peptide hydrogel fosters chondrocyte extracellular matrix production and cell division: implications for cartilage tissue repair. Proc Natl Acad Sci U S A **99,** 9996, 2002.
18. Mann, B.K., Schmedlen, R.H., and West, J.L. Tethered-TGF-β increases extracellular matrix production of vascular smooth muscle cells. Biomaterials **22,** 439, 2001.
19. Zeltinger, J., Sherwood, J.K., Graham, D.A., Mueller, R., and Griffith, L.G. Effect of pore size and void fraction on cellular adhesion, proliferation, and matrix deposition. Tissue Eng **7,** 557, 2001.
20. Duymaz, B.T., Erdiler, F.B., Alan, T., et al. 3D bioprinting of levan/polycaprolactone/gelatin blends for bone tissue engineering: characterization of the cellular behavior. Eur Polym J **119,** 426, 2019.
21. Holzl, K., Lin, S.M., Tytgat, L., Van Vlierberghe, S., Gu, L.X., and Ovsianikov, A. Bioink properties before, during and after 3D bioprinting. Biofabrication **8,** 032002, 2016.
22. Deo, K.A., Lokhande, G., and Gaharwar, A.K. Nanostructured hydrogels for tissue engineering and regenerative medicine. In: Reis R.L., ed. Encyclopedia of Tissue Engineering and Regenerative Medicine. Oxford, Unted Kingdom: Academic Press, 2019, pp. 21.
23. Trachsel, L., Johnbosco, C., Lang, T., Benetti, E.M., and Zenobi-Wong, M. Double-network hydrogels including enzymatically crosslinked poly-(2-alkyl-2-oxazoline)s for 3D bioprinting of cartilage-engineering constructs. Biomacromolecules **20,** 4502, 2019.
24. Si, H.P., Xing, T.L., Ding, Y.L., Zhang, H.B., Yin, R.X., and Zhang, W.J. 3D bioprinting of the sustained drug release wound dressing with double-crosslinked hyaluronic-acid-based hydrogels. Polymers **11,** 21, 2019.
25. Huang, J., Fu, H., Wang, Z., et al. BMSCs-laden gelatin/sodium alginate/carboxymethyl chitosan hydrogel for 3D bioprinting. RSC Adv **6,** 108423, 2016.
26. Hong, S., Kim, J.S., Jung, B., Won, C., and Hwang, C. Coaxial bioprinting of cell-laden vascular constructs using a gelatin–tyramine bioink. Biomater Sci **7,** 4578, 2019.
27. Zhang, B., Gao, L., Gu, L., Yang, H., Luo, Y., and Ma, L. High-resolution 3D bioprinting system for fabricating cell-laden hydrogel scaffolds with high cellular activities. Proc CIRP **65,** 219, 2017.

28. Nair, K., Gandhi, M., Khalil, S., *et al*. Characterization of cell viability during bioprinting processes. Biotechnol J **4,** 1168, 2009.

29. Kolesky, D.B., Homan, K.A., Skylar-Scott, M.A., and Lewis, J.A. Three-dimensional bioprinting of thick vascularized tissues. Proc Natl Acad Sci U S A **113,** 3179, 2016.

30. Colosi, C., Shin, S.R., Manoharan, V., *et al*. Microfl uidic bioprinting of heterogeneous 3D tissue constructs using low-viscosity bioink. Adv Mater **28,** 677, 2016.

31. Tigner, T.J., Rajput, S., Gaharwar, A.K., and Alge, D.L. Comparison of photo cross linkable gelatin derivatives and initiators for three-dimensional extrusion bioprinting. Biomacromolecules **21,** 454, 2020.

32. Kim, M.H., Lee, Y.W., Jung, W.K., Oh, J., and Nam, S.Y. Enhanced rheological behaviors of alginate hydrogels with carrageenan for extrusion-based bioprinting. J Mech Behav Biomed Mater **98,** 187, 2019.

33. Singh, Y.P., Bandyopadhyay, A., and Mandal, B.B. 3D bioprinting using cross-linker-free silk-gelatin bioink for cartilage tissue engineering. ACS Appl Mater Interfaces **11,** 33684, 2019.

34. Xu, C., Lee, W., Dai, G., and Hong, Y. Highly elastic biodegradable single-network hydrogel for cell printing. ACS Appl Mater Interfaces **10,** 9969, 2018.

35. Ying, G., Jiang, N., Yu, C., and Zhang, Y.S. Three-dimensional bioprinting of gelatin methacryloyl (GelMA). Biodes Manuf **1,** 215, 2018.

36. Yin, J., Yan, M., Wang, Y., Fu, J., and Suo, H. 3D bioprinting of low-concentration cell-laden gelatin methacrylate (GelMA) bioinks with a two-step cross-linking strategy. ACS Appl Mater Interfaces **10,** 6849, 2018.

37. Nguyen, D., Hägg, D.A., Forsman, A., *et al*. Cartilage tissue engineering by the 3D bioprinting of iPS cells in a nanocellulose/alginate bioink. Sci Rep **7,** 658, 2017.

38. Bendtsen, S.T., Quinnell, S.P., and Wei, M. Development of a novel alginate-polyvinyl alcohol-hydroxyapatite hydrogel for 3D bioprinting bone tissue engineered scaffolds. J Biomed Mater Res A **105,** 1457, 2017.

39. Paxton, N., Smolan, W., Böck, T., Melchels, F., Groll, J., and Jungst, T. Proposal to assess printability of bioinks for extrusion-based bioprinting and evaluation of rheological properties governing bioprintability. Biofabrication **9,** 044107, 2017.

40. Chimene, D., Kaunas, R., and Gaharwar, A.K. Hydrogel bioink reinforcement for additive manufacturing: a focused review of emerging strategies. Adv Mater **32,** e1902026, 2020.

41. Raddatz, L., Lavrentieva, A., Pepelanova, I., *et al*. Development and application of an additively manufactured calcium chloride nebulizer for alginate 3D-bioprinting purposes. J Func Biomater **9,** 14, 2018.

42. Smith, C.M., Stone, A.L., Parkhill, R.L., *et al*. Three-dimensional bioassembly tool for generating viable tissue-engineered constructs. Tissue Eng **10,** 1566, 2004.

43. Campos, D.F.D., Blaeser, A., Weber, M., *et al*. Three-dimensional printing of stem cell-laden hydrogels submerged in a hydrophobic high-density fluid. Biofabrication **5,** 015003, 2012.

44. Ouyang, L., Highley, C.B., Sun, W., and Burdick, J.A. A Generalizable strategy for the 3D bioprinting of hydrogels from nonviscous photo-crosslinkable inks. Adv Mater **29,** 1604983, 2017.

45. Chang, R., Nam, J., and Sun, W. Effects of dispensing pressure and nozzle diameter on cell survival from solid freeform fabrication–based direct cell writing. Tissue Eng Part A **14,** 41, 2008.

46. Marga, F., Jakab, K., Khatiwala, C., *et al*. Toward engineering functional organ modules by additive manufacturing. Biofabrication **4,** 022001, 2012.

47. Serna, J.A., Florez, S.L., Talero, V.A., Briceno, J.C., Munoz-Camargo, C., and Cruz, J.C. Formulation and characterization of a SIS-based photocrosslinkable bioink. Polymers **11,** 10, 2019.

48. Freeman, S., Ramos, R., Chando, P.A., *et al*. A bioink blend for rotary 3D bioprinting tissue engineered small-diameter vascular constructs. Acta Biomater **95,** 152, 2019.

49. Miguel, S.P., Cabral, C.S.D., Moreira, A.F., and Correia, I.J. Production and characterization of a novel asymmetric 3D printed construct aimed for skin tissue regeneration. Colloids Surf B Biointerfaces **181,** 994, 2019.

50. Blaeser, A., Campos, D.F.D., Puster, U., Richtering, W., Stevens, M.M., and Fischer, H. Controlling shear stress in 3D bioprinting is a key factor to balance printing resolution and stem cell integrity. Adv Healthc Mater **5,** 326, 2016.

51. Anil Kumar, S., Alonzo, M., Allen, S.C., *et al*. A visible light-cross-linkable, fibrin–gelatin-based bioprinted construct with human cardiomyocytes and fibroblasts. ACS Biomater Sci Eng **5,** 4551, 2019.

52. Dubbin, K., Hori, Y., Lewis, K.K., and Heilshorn, S.C. Dual-stage crosslinking of a gel-phase bioink improves cell viability and homogeneity for 3D bioprinting. Adv Healthc Mater **5,** 2488, 2016.

53. Zhao, Y., Li, Y., Mao, S., Sun, W., and Yao, R. The influence of printing parameters on cell survival rate and printability in microextrusion-based 3D cell printing technology. Biofabrication **7,** 045002, 2015.

54. Ouyang, L., Yao, R., Chen, X., Na, J., and Sun, W. 3D printing of HEK 293FT cell-laden hydrogel into macroporous constructs with high cell viability and normal biological functions. Biofabrication **7,** 015010, 2015.

55. Zhu, W., Qu, X., Zhu, J., *et al*. Direct 3D bioprinting of prevascularized tissue constructs with complex microarchitecture. Biomaterials **124,** 106, 2017.

56. Mishbak, H.H., Cooper, G., and Bartolo, P.J. Development and characterization of a photocurable alginate bioink for three-dimensional bioprinting. Int J Bioprinting **5,** 12, 2019.

57. Thakur, A., Jaiswal, M.K., Peak, C.W., *et al*. Injectable shear-thinning nanoengineered hydrogels for stem cell delivery. Nanoscale **8,** 12362, 2016.

58. Basu, S., Pacelli, S., Feng, Y., Lu, Q., Wang, J., and Paul, A. Harnessing the noncovalent interactions of DNA backbone with 2D silicate nanodisks to fabricate injectable therapeutic hydrogels. ACS Nano **12,** 9866, 2018.

59. Lokhande, G., Carrow, J.K., Thakur, T., *et al*. Nanoengineered injectable hydrogels for wound healing application. Acta Biomater **70,** 35, 2018.

60. Saha, K., Keung, A.J., Irwin, E.F., *et al*. Substrate modulus directs neural stem cell behavior. Biophys J **95,** 4426, 2008.

61. Tse, J.R., and Engler, A.J. Stiffness gradients mimicking in vivo tissue variation regulate mesenchymal stem cell fate. PLoS One **6,** e15978, 2011.

62. Pek, Y.S., Wan, A.C.A., and Ying, J.Y. The effect of matrix stiffness on mesenchymal stem cell differentiation in a 3D thixotropic gel. Biomaterials **31,** 385, 2010.

63. Cruise, G.M., Scharp, D.S., and Hubbell, J.A. Characterization of permeability and network structure of interfacially photopolymerized poly(ethylene glycol) diacrylate hydrogels. Biomaterials **19,** 1287, 1998.

64. Dikovsky, D., Bianco-Peled, H., and Seliktar, D. The effect of structural alterations of PEG-fibrinogen hydrogel scaffolds on 3-D cellular morphology and cellular migration. Biomaterials **27,** 1496, 2006.

65. Liu, W., Heinrich, M.A., Zhou, Y., *et al.* Extrusion bioprinting of shear-thinning gelatin methacryloyl bioinks. Adv Healthc Mater **6,** 1601451, 2017.

66. Gaharwar, A.K., Avery, R.K., Assmann, A., *et al.* Shear-thinning nanocomposite hydrogels for the treatment of hemorrhage. ACS Nano **8,** 9833, 2014.

67. He, Y., Yang, F.F., Zhao, H.M., Gao, Q., Xia, B., and Fu, J.Z. Research on the printability of hydrogels in 3D bioprinting. Sci Rep **6,** 29977, 2016.

68. Jia, J., Richards, D.J., Pollard, S., *et al.* Engineering alginate as bioink for bioprinting. Acta Biomater **10,** 4323, 2014.

69. Husseman, M., Malmstrom, E.E., McNamara, M., *et al.* Controlled synthesis of polymer brushes by ''Living'' free radical polymerization techniques. Macromolecules **32,** 1424, 1999.

70. Tayal, A., Kelly, R.M., and Khan, S.A. Rheology and molecular weight changes during enzymatic degradation of a water-soluble polymer. Macromolecules **32,** 294, 1999.

71. Bryant, S.J., and Anseth, K.S. Controlling the spatial distribution of ECM components in degradable PEG hydrogels for tissue engineering cartilage. J Biomed Mater Res A **64A,** 70, 2003.

72. Zhu, J.M. Bioactive modification of poly(ethylene glycol) hydrogels for tissue engineering. Biomaterials **31,** 4639, 2010.

73. Mironov, V., Visconti, R.P., Kasyanov, V., Forgacs, G., Drake, C.J., and Markwald, R.R. Organ printing: tissue spheroids as building blocks. Biomaterials **30,** 2164, 2009.

74. Ji, S., Dube, K., Chesterman, J.P., *et al.* Polyester-based ink platform with tunable bioactivity for 3D printing of tissue engineering scaffolds. Biomater Sci **7,** 560, 2019.

75. Ma, X.Y., Yu, C., Wang, P.R., *et al.* Rapid 3D bioprinting of decellularized extracellular matrix with regionally varied mechanical properties and biomimetic microarchitecture. Biomaterials **185,** 310, 2018.

76. Ferreira, D.S., Lin, Y.A., Cui, H.G., Hubbell, J.A., Reis, R.L., and Azevedo, H.S. Molecularly engineered self-assembling membranes for cell-mediated degradation. Adv Healthc Mater **4,** 602, 2015.

77. Rodell, C.B., Wade, R.J., Purcell, B.P., Dusaj, N.N., and Burdick, J.A. Selective proteolytic degradation of guest-host assembled, injectable hyaluronic acid hydrogels. ACS Biomater Sci Eng **1,** 277, 2015.

78. Jivan, F., Yegappan, R., Pearce, H., *et al.* Sequential thiol–ene and tetrazine click reactions for the polymerization and functionalization of hydrogel microparticles. Biomacromolecules **17,** 3516, 2016.

79. Jaiswal, M.K., Carrow, J.K., Gentry, J.L., *et al.* Vacancy-driven gelation using defect-rich nanoassemblies of 2D transition metal dichalcogenides and polymeric binder for biomedical applications. Adv Mater **29,** 1702037, 2017.

80. Censi, R., Schuurman, W., Malda, J., *et al.* A printable photopolymerizable thermosensitive p(HPMAm-lactate)-PEG hydrogel for tissue engineering. Adv Funct Mater **21,** 1833, 2011.

81. Kesti, M., Müller, M., Becher, J., *et al.* A versatile bioink for three-dimensional printing of cellular scaffolds based on thermally and photo-triggered tandem gelation. Acta Biomater **11,** 162, 2015.

82. Guttman, C.M., and Dimarzio, E.A. Polymer separation by flow and its relation to GPC. Bull Am Phys Soc **14,** 424, 1969.

83. Balke, S.T., and Hamielec, A.E. Polymer reactors and molecular weight distribution. 8. A method of interpreting skewed GPC chromatograms. J Appl Polym Sci **13,** 1381, 1969.

84. Mouser, V.H.M., Abbadessa, A., Levato, R., *et al.* Development of a thermosensitive HAMA-containing bioink for the fabrication of composite cartilage repair constructs. Biofabrication **9,** 015026, 2017.

85. Shin, M., Galarraga, J.H., Kwon, M.Y., Lee, H., and Burdick, J.A. Gallol-derived ECM-mimetic adhesive bioinks exhibiting temporal shear-thinning and stabilization behavior. Acta Biomater **95,** 165, 2019.

86. Bertlein, S., Brown, G., Lim, K.S., *et al.* Thiol–ene clickable gelatin: a platform bioink for multiple 3D biofabrication technologies. Adv Mater **29,** 1703404, 2017.

87. Gao, T., Gillispie, G.J., Copus, J.S., *et al.* Optimization of gelatin–alginate composite bioink printability using rheological parameters: a systematic approach. Biofabrication **10,** 034106, 2018.

88. Jessop, Z.M., Al-Sabah, A., Gao, N., *et al.* Printability of pulp derived crystal, fibril and blend nanocellulose-alginate bioinks for extrusion 3D bioprinting. Biofabrication **11,** 16, 2019.

89. Ouyang, L., Yao, R., Zhao, Y., and Sun, W. Effect of bioink properties on printability and cell viability for 3D bioplotting of embryonic stem cells. Biofabrication **8,** 035020, 2016.

90. Axpe, E., and Oyen, M.L. Applications of alginate-based bioinks in 3D bioprinting. Int J Mol Sci **17,** 1976, 2016.

91. Diamantides, N., Wang, L., Pruiksma, T., *et al.* Correlating rheological properties and printability of collagen bioinks: the effects of riboflavin photocrosslinking and pH. Biofabrication **9,** 034102, 2017.

92. Melchels, F.P., Dhert, W.J., Hutmacher, D.W., and Malda, J. Development and characterisation of a new bioink for additive tissue manufacturing. J Mater Chem B **2,** 2282, 2014.

93. Yeh, Y.-C., Highley, C.B., Ouyang, L., and Burdick, J.A. 3D printing of photocurable poly (glycerol sebacate) elastomers. Biofabrication **8,** 045004, 2016.

94. Schuurman, W., Levett, P.A., Pot, M.W., *et al.* Gelatin-methacrylamide hydrogels as potential biomaterials for fabrication of tissue-engineered cartilage constructs. Macromol Biosci **13,** 551, 2013.

95. Jaiswal, M.K., Xavier, J.R., Carrow, J.K., Desai, P., Alge, D., and Gaharwar, A.K. Mechanically stiff nanocomposite hydrogels at ultralow nanoparticle content. ACS Nano **10,** 246, 2015.

96. Gaharwar, A.K., Cross, L.M., Peak, C.W., *et al.* 2D nanoclay for biomedical applications: regenerative medicine, therapeutic delivery, and additive manufacturing. Adv Mater **31,** 1900332, 2019.

97. Chimene, D., Miller, L., Cross, L., Jaiswal, M.K., Singh, I., Gaharwar, A.K. Nanoengineered osteoinductive bioink for 3D bioprinting bone tissue. ACS Appl Mater Interfaces 2020. [Epub ahead of print]; DOI: 10.1021/acsami.9b19037.

98. Rutz, A.L., Hyland, K.E., Jakus, A.E., Burghardt, W.R., and Shah, R.N. A multimaterial bioink method for 3D printing tunable, cell-compatible hydrogels. Adv Mater **27,** 1607, 2015.

99. Suntornnond, R., Tan, E., An, J., and Chua, C. A mathematical model on the resolution of extrusion bioprinting for the development of new bioinks. Materials **9,** 756, 2016.

100. Aguado, B.A., Mulyasasmita, W., Su, J., Lampe, K.J., and Heilshorn, S.C. Improving viability of stem cells during syringe needle flow through the design of hydrogel cell carriers. Tissue Eng Part A **18,** 806, 2012.

101. Highley, C.B., Rodell, C.B., and Burdick, J.A. Direct 3D printing of shear-thinning hydrogels into self-healing hydrogels. Adv Mater **27,** 5075, 2015.

102. Li, H.J., Liu, S.J., and Li, L. Rheological study on 3D printability of alginate hydrogel and effect of graphene oxide. Int J Bioprinting **2,** 54, 2016.

103. Leone, G., Torricelli, P., Chiumiento, A., Facchini, A., and Barbucci, R. Amidic alginate hydrogel for nucleus pulposus replacement. J Biomed Mater Res A **84,** 391, 2008.

104. Bandyopadhyay, A., and Mandal, B.B. A three-dimensional printed silk-based biomimetic tri-layered meniscus for potential patient-specific implantation. Biofabrication **12,** 015003, 2019.

105. Chen, D.X.B. Preparation of Scaffold solutions and characterization of their flow behavior. In: Extrusion Bioprinting of Scaffolds for Tissue Engineering Applications. Cham, Switzerland: Springer International Publishing, 2019, pp. 91.

106. Critchley, S.E., and Kelly, D.J. Bioinks for bioprinting functional meniscus and articular cartilage. J 3D Print Med **1,** 269, 2017.

107. Lorson, T., Jaksch, S., Lübtow, M.M., et al. A thermogelling supramolecular hydrogel with sponge-like morphology as a cytocompatible bioink. Biomacromolecules **18,** 2161, 2017.

108. Glassman, M.J., and Olsen, B.D. Structure and mechanical response of protein hydrogels reinforced by block copolymer self-assembly. Soft Matter **9,** 6814, 2013.

109. Glassman, M.J., Chan, J., and Olsen, B.D. Reinforcement of shear thinning protein hydrogels by responsive block copolymer self-assembly. Adv Funct Mater **23,** 1182, 2013.

110. Senff, H., and Richtering, W. Temperature sensitive microgel suspensions: colloidal phase behavior and rheology of soft spheres. J Chem Phys **111,** 1705, 1999.

111. Beck, E.C., Barragan, M., Tadros, M.H., et al. Chondroinductive hydrogel pastes composed of naturally derived devitalized cartilage. Ann Biomed Eng **44,** 1863, 2016.

112. Ribeiro, A., Blokzijl, M.M., Levato, R., et al. Assessing bioink shape fidelity to aid material development in 3D bioprinting. Biofabrication **10,** 014102, 2017.

113. Peak, C.W., Stein, J., Gold, K.A., and Gaharwar, A.K. Nanoengineered colloidal inks for 3D bioprinting. Langmuir **34,** 917, 2018.

114. Cofino, C., Perez-Amodio, S., Semino, C.E., Engel, E., and Mateos-Timoneda, M.A. Development of a self-assembled peptide/methylcellulose-based bioink for 3D bioprinting. Macromol Mater Eng **304,** 9, 2019.

115. Alruwaili, M., Lopez, J.A., McCarthy, K., Reynaud, E.G., and Rodriguez, B.J. Liquid-phase 3D bioprinting of gelatin alginate hydrogels: influence of printing parameters on hydrogel line width and layer height. Biodes Manuf **2,** 172, 2019.

116. Shim, J.-H., Kim, J.Y., Park, M., Park, J., and Cho, D.-W. Development of a hybrid scaffold with synthetic biomaterials and hydrogel using solid freeform fabrication technology. Biofabrication **3,** 034102, 2011.

117. Zhang, Y.S., Yue, K., Aleman, J., et al. 3D bioprinting for tissue and organ fabrication. Ann Biomed Eng **45,** 148, 2017.

118. Hockaday, L.A., Kang, K.H., Colangelo, N.W., et al. Rapid 3D printing of anatomically accurate and mechanically heterogeneous aortic valve hydrogel scaffolds. Biofabrication **4,** 035005, 2012.

119. Pawlaczyk, M., Lelonkiewicz, M., and Wieczorowski, M. Age-dependent biomechanical properties of the skin. Postepy Dermatol Alergol **30,** 302, 2013.

120. Rho, J.Y., Ashman, R.B., and Turner, C.H. Young's modulus of trabecular and cortical bone material: ultrasonic and microtensile measurements. J Biomech **26,** 111, 1993.

121. Muiznieks, L.D., and Keeley, F.W. Molecular assembly and mechanical properties of the extracellular matrix: a fibrous protein perspective. Biochim Biophys Acta **1832,** 866, 2013.

122. Roohani-Esfahani, S.-I., Newman, P., and Zreiqat, H. Design and fabrication of 3D printed scaffolds with a mechanical strength comparable to cortical bone to repair large bone defects. Sci Rep **6,** 19468, 2016.

123. El-Hajje, A., Kolos, E.C., Wang, J.K., et al. Physical and mechanical characterisation of 3D-printed porous titanium for biomedical applications. J Mater Sci Mater Med **25,** 2471, 2014.

124. Morley, C.D., Ellison, S.T., Bhattacharjee, T., et al. Quantitative characterization of 3D bioprinted structural elements under cell generated forces. Nat Commun **10,** 9, 2019.

125. Johnson, B.D., Beebe, D.J., and Crone, W.C. Effects of swelling on the mechanical properties of a pH-sensitive hydrogel for use in microfluidic devices. Mater Sci Eng C **24,** 575, 2004.

126. Caló, E., and Khutoryanskiy, V.V. Biomedical applications of hydrogels: a review of patents and commercial products. Eur Polym J **65,** 252, 2015.

127. Peak, C.W., Carrow, J.K., Thakur, A., Singh, A., and Gaharwar, A.K. Elastomeric cell-laden nanocomposite microfibers for engineering complex tissues. Cell Mol Bioeng **8,** 404, 2015.

128. Anderson, J.M., and Shive, M.S. Biodegradation and biocompatibility of PLA and PLGA microspheres. Adv Drug Deliv Rev **28,** 5, 1997.

129. Danhier, F., Ansorena, E., Silva, J.M., Coco, R., Le Breton, A., and Preat, V. PLGA-based nanoparticles: an overview of biomedical applications. J Control Release **161,** 505, 2012.

130. Freiberg, S., and Zhu, X. Polymer microspheres for controlled drug release. Int J Pharm **282,** 1, 2004.

131. Makadia, H.K., and Siegel, S.J. Poly lactic-co-glycolic acid (PLGA) as biodegradable controlled drug delivery carrier. Polymers **3,** 1377, 2011.

132. Peak, C.W., Nagar, S., Watts, R.D., and Schmidt, G. Robust and degradable hydrogels from poly(ethylene glycol) and semi-interpenetrating collagen. Macromolecules **47,** 6408, 2014.

133. Dai, X.S., Chen, X., Yang, L., Foster, S., Coury, A.J., and Jozefiak, T.H. Free radical polymerization of poly(ethylene glycol) diacrylate macromers: impact of macromer hydrophobicity and initiator chemistry on polymerization efficiency. Acta Biomater **7,** 1965, 2011.

134. Guarino, V., Gloria, A., De Santis, R., and Ambrosio, L. Composite hydrogels for scaffold design, tissue engineering, and prostheses. 2010.

135. Cushing, M.C., and Anseth, K.S. Hydrogel cell cultures. Science **316,** 1133, 2007.

136. Gao, G., Schilling, A.F., Yonezawa, T., Wang, J., Dai, G., and Cui, X. Bioactive nanoparticles stimulate bone tissue formation in bioprinted three-dimensional scaffold and human mesenchymal stem cells. Biotechnol J **9,** 1304, 2014.

137. Skardal, A., Zhang, J., McCoard, L., Oottamasathien, S., and Prestwich, G.D. Dynamically crosslinked gold nanoparticle–hyaluronan hydrogels. Adv Mater **22,** 4736, 2010.

138. Jia, W.T., Gungor-Ozkerim, P.S., Zhang, Y.S., *et al*. Direct 3D bioprinting of perfusable vascular constructs using a blend bioink. Biomaterials **106,** 58, 2016.

139. Sun, Y., You, Y.Q., Jiang, W.B., Zhai, Z.J., and Dai, K.R. 3D-bioprinting a genetically inspired cartilage scaffold with GDF5-conjugated BMSC-laden hydrogel and polymer for cartilage repair. Theranostics **9,** 6949, 2019.

140. Chen, N., Zhu, K., Zhang, Y.S., *et al*. Hydrogel bioink with multilayered interfaces improves dispersibility of encapsulated cells in extrusion bioprinting. ACS Appl Mater Interfaces **11,** 30585, 2019.

141. Smith, R.L., Carter, D.R., and Schurman, D.J. Pressure and shear differentially alter human articular chondrocyte metabolism—a review. Clin Orthop Relat Res S89, 2004.

142. Zhao, F., Chella, R., and Ma, T. Effects of shear stress on 3-D human mesenchymal stem cell construct development in a perfusion bioreactor system: experiments and hydrodynamic modeling. Biotechnol Bioeng **96,** 584, 2007.

143. Billiet, T., Gevaert, E., De Schryver, T., Cornelissen, M., and Dubruel, P. The 3D printing of gelatin methacrylamide cell-laden tissue-engineered constructs with high cell viability. Biomaterials **35,** 49, 2014.

144. Kolesky, D.B., Truby, R.L., Gladman, A.S., Busbee, T.A., Homan, K.A., and Lewis, J.A. 3D bioprinting of vascularized, heterogeneous cell-laden tissue constructs. Adv Mater **26,** 3124, 2014.

145. Xavier, J.R., Thakur, T., Desai, P., *et al*. Bioactive nanoengineered hydrogels for bone tissue engineering: a growth-factor-free approach. ACS Nano **9,** 3109, 2015.

146. Yang, J.Z., Zhang, Y.S., Yue, K., and Khademhosseini, A. Cell-laden hydrogels for osteochondral and cartilage tissue engineering. Acta Biomater **57,** 1, 2017.

147. Gao, G.F., Schilling, A.F., Hubbell, K., *et al*. Improved properties of bone and cartilage tissue from 3D inkjet-bioprinted human mesenchymal stem cells by simultaneous deposition and photocrosslinking in PEG-GelMA. Biotechnol Lett **37,** 2349, 2015.

148. Sawkins, M.J., Mistry, P., Brown, B.N., Shakesheff, K.M., Bonassar, L.J., and Yang, J. Cell and protein compatible 3D bioprinting of mechanically strong constructs for bone repair. Biofabrication **7,** 035004, 2015.

149. Raphael, B., Khalil, T., Workman, V.L., *et al*. 3D cell bioprinting of self-assembling peptide-based hydrogels. Mater Lett **190,** 103, 2017.

150. Loo, Y.H., and Hauser, C.A.E. Bioprinting synthetic self-assembling peptide hydrogels for biomedical applications. Biomed Mater **11,** 014103, 2015.

151. Loo, Y.H., Lakshmanan, A., Ni, M., Toh, L.L., Wang, S., and Hauser, C.A.E. Peptide bioink: self-assembling nanofibrous scaffolds for three-dimensional organotypic cultures. Nano Lett **15,** 6919, 2015.

152. Kundu, J., Shim, J.H., Jang, J., Kim, S.W., and Cho, D.W. An additive manufacturing-based PCL-alginate-chondrocyte bioprinted scaffold for cartilage tissue engineering. J Tissue Eng Regen Med **9,** 1286, 2015.

153. Carrow, J. K., Di Luca, A., Dolatshahi-Pirouz, A., Moroni, L., and Gaharwar, A. K. 3D-printed bioactive scaffolds from nanosilicates and PEOT/PBT for bone tissue engineering. Regen Biomater **6,** 29, 2019.

154. Zhang, K.L., Fu, Q., Yoo, J., *et al*. 3D bioprinting of urethra with PCL/PLCL blend and dual autologous cells in fibrin hydrogel: an in vitro evaluation of biomimetic mechanical property and cell growth environment. Acta Biomater **50,** 154, 2017.

155. Bakarich, S.E., Balding, P., Gorkin, R., Spinks, G.M., and Panhuis, M.I.H. Printed ionic-covalent entanglement hydrogels from carrageenan and an epoxy amine. RSC Adv **4,** 38088, 2014.

156. Choi, B., Park, K.S., Kim, J.H., *et al*. Stiffness of hydrogels regulates cellular reprogramming efficiency through mesenchymal-to-epithelial transition and stemness markers. Macromol Biosci **16,** 199, 2016.

157. Birkholz, M.N., Agrawal, G., Bergmann, C., *et al*. Calcium phosphate/microgel composites for 3D powderbed printing of ceramic materials. Biomed Tech (Berl) **61,** 267, 2016.

158. Hinton, T.J., Hudson, A., Pusch, K., Lee, A., and Feinberg, A.W. 3D printing PDMS elastomer in a hydrophilic support bath via freeform reversible embedding. ACS Biomater Sci Eng **2,** 1781, 2016.

159. Lee, K.Y., and Mooney, D.J. Alginate: properties and biomedical applications. Prog Polym Sci **37,** 106, 2012.

160. Rutz, A.L., Gargus, E.S., Hyland, K.E., *et al*. Employing PEG crosslinkers to optimize cell viability in gel phase bioinks and tailor post printing mechanical properties. Acta Biomater **99,** 121, 2019.

161. Discher, D.E., Janmey, P., and Wang, Y.L. Tissue cells feel and respond to the stiffness of their substrate. Science **310,** 1139, 2005.

162. Ahmad Khalili, A., and Ahmad, M.R. A review of cell adhesion studies for biomedical and biological applications. Int J Mol Sci **16,** 18149, 2015.

163. Aigner, T., Neureiter, D., Muller, S., Kuspert, G., Belke, J., and Kirchner, T. Extracellular matrix composition and gene expression in collagenous colitis. Gastroenterology **113,** 136, 1997.

164. Kass, L., Erler, J.T., Dembo, M., and Weaver, V.M. Mammary epithelial cell: influence of extracellular matrix composition and organization during development and tumorigenesis. Int J Biochem Cell Biol **39,** 1987, 2007.

165. Sulzer, M.A., Leers, M.P., van Noord, J.A., Bollen, E.C., and Theunissen, P.H. Reduced E-cadherin expression is associated with increased lymph node metastasis and unfavorable prognosis in non-small cell lung cancer. Am J Respir Crit Care Med **157,** 1319, 1998.

166. van Gurp, R.J., Oosterhuis, J.W., Kalscheuer, V., Mariman, E.C., and Looijenga, L.H. Biallelic expression of the H19 and IGF2 genes in human testicular germ cell tumors. J Natl Cancer Inst **86,** 1070, 1994.

167. Huang, S., and Ingber, D.E. The structural and mechanical complexity of cell-growth control. Nat Cell Biol **1,** E131, 1999.

168. Zhou, B., Heider, Y., Ma, S.Y., and Markert, B. Phase-field-based modelling of the gelation process of biopolymer droplets in 3D bioprinting. Comput Mech **63,** 1187, 2019.

169. Dembo, M., and Wang, Y.-L. Stresses at the cell-to-substrate interface during locomotion of fibroblasts. Biophys J **76,** 2307, 1999.

170. Kraning-Rush, C.M., Califano, J.P., and Reinhart-King, C.A. Cellular traction stresses increase with increasing metastatic potential. PLoS One **7,** e32572, 2012.

171. Wang, X.F., Lu, P.J., Song, Y., Sun, Y.C., Wang, Y.G., and Wang, Y. Nano hydroxyapatite particles promote osteogenesis in a three-dimensional bio-printing construct consisting of alginate/gelatin/hASCs. RSC Adv **6,** 6832, 2016.

172. Fraley, S.I., Feng, Y., Krishnamurthy, R., et al. A distinctive role for focal adhesion proteins in three-dimensional cell motility. Nat Cell Biol **12,** 598, 2010.

173. Thomas, G., Burnham, N.A., Camesano, T.A., and Wen, Q. Measuring the mechanical properties of living cells using atomic force microscopy. J Vis Exp **76,** e50497, 2013.

174. Paul, K., Darzi, S., McPhee, G., et al. 3D bioprinted endometrial stem cells on melt electrospun poly epsilon-caprolactone mesh for pelvic floor application promote anti-inflammatory responses in mice. Acta Biomater **97,** 162, 2019.

175. Daviran, M., Caram, H.S., and Schultz, K.M. Role of cell-mediated enzymatic degradation and cytoskeletal tension on dynamic changes in the rheology of the pericellular region prior to human mesenchymal stem cell motility. ACS Biomater Sci Eng **4,** 468, 2018.

176. Daviran, M., Longwill, S.M., Casella, J.F., and Schultz, K.M. Rheological characterization of dynamic remodeling of the pericellular region by human mesenchymal stem cell-secreted enzymes in well-defined synthetic hydrogel scaffolds. Soft Matter **14,** 3078, 2018.

177. Schultz, K.M., Kyburz, K.A., and Anseth, K.S. Measuring dynamic cell–material interactions and remodeling during 3D human mesenchymal stem cell migration in hydrogels. Proc Natl Acad Sci U S A **112,** E3757, 2015.

178. Kirker, K.R., Luo, Y., Nielson, J.H., Shelby, J., and Prestwich, G.D. Glycosaminoglycan hydrogel films as bio-interactive dressings for wound healing. Biomaterials **23,** 3661, 2002.

179. Woessner, J.F. The determination of hydroxyproline in tissue and protein samples containing small proportions of this imino acid. Arch Biochem Biophys **93,** 440, 1961.

180. Walsh, B.J., Thornton, S.C., Penny, R., and Breit, S.N. Microplate reader-based quantitation of collagens. Anal Biochem **203,** 187, 1992.

181. Bitter, T., and Muir, H.M. A modified uronic acid carbazole reaction. Anal Biochem **4,** 330, 1962.

182. Frazier, S.B., Roodhouse, K.A., Hourcade, D.E., and Zhang, L. The quantification of glycosaminoglycans: a comparison of HPLC, carbazole, and alcian blue methods. Open Glycosci **1,** 31, 2008.

183. Barbosa, I., Garcia, S., Barbier-Chassefière, V., Caruelle, J.-P., Martelly, I., and Papy-García, D. Improved and simple micro assay for sulfated glycosaminoglycans quantification in biological extracts and its use in skin and muscle tissue studies. Glycobiology **13,** 647, 2003.

184. McLeod, C.M., and Mauck, R.L. High fidelity visualization of cell-to-cell variation and temporal dynamics in nascent extracellular matrix formation. Sci Rep **6,** 38852, 2016.

185. Loebel, C., Mauck, R.L., and Burdick, J.A. Local nascent protein deposition and remodelling guide mesenchymal stromal cell mechanosensing and fate in three-dimensional hydrogels. Nat Mater **18,** 883, 2019.

186. Liu, W., Zhang, Y.S., Heinrich, M.A., et al. Rapid continuous multimaterial extrusion bioprinting. Adv Mater **29,** 1604630, 2017.

187. Van Belleghem, S., Torres, L., Santoro, M., et al. Hybrid 3D printing of synthetic and cell-laden bioinks for shape retaining soft tissue grafts. Adv Funct Mater **30,** 1907145, 2020.

188. Rocca, M., Fragasso, A., Liu, W.J., Heinrich, M.A., and Zhang, Y.S. Embedded multimaterial extrusion bioprinting. SLAS Technol **23,** 154, 2018.

189. Serex, L., Bertsch, A., and Renaud, P. Microfluidics: a new layer of control for extrusion-based 3D printing. Micromachines **9,** 11, 2018.

190. Joung, D., Truong, V., Neitzke, C.C., et al. 3D printed stem-cell derived neural progenitors generate spinal cord scaffolds. Adv Funct Mater **28,** 10, 2018.

191. de Rutte, J.M., Koh, J., and Di Carlo, D. Scalable high-throughput production of modular microgels for in situ assembly of microporous tissue scaffolds. Adv Funct Mater **29,** 10, 2019.

192. Idaszek, J., Costantini, M., Karlsen, T.A., et al. 3D bioprinting of hydrogel constructs with cell and material gradients for the regeneration of full-thickness chondral defect using a microfluidic printing head. Biofabrication **11,** 15, 2019.

193. Han, X., Bibb, R., and Harris, R. Engineering design of artificial vascular junctions for 3D printing. Biofabrication **8,** 025018, 2016.

194. Gold, K., Gaharwar, A.K., and Jain, A. Emerging trends in multiscale modeling of vascular pathophysiology: organ-on-a-chip and 3D printing. Biomaterials **196,** 2, 2019.

195. Jang, J., Yi, H.-G., and Cho, D.-W. 3D printed tissue models: present and future. ACS Biomater Sci Eng **2,** 1722, 2016.

196. Nguyen, D.G., Funk, J., Robbins, J.B., et al. Bioprinted 3D primary liver tissues allow assessment of organ-level response to clinical drug induced toxicity in vitro. PLoS One **11,** 17, 2016.

197. Li, H., Fan, X., and Houghton, J. Tumor microenvironment: the role of the tumor stroma in cancer. J Cell Biochem **101,** 805, 2007.

198. Xu, F., Celli, J., Rizvi, I., Moon, S., Hasan, T., and Demirci, U. A three-dimensional in vitro ovarian cancer coculture model using a high-throughput cell patterning platform. Biotechnol J **6,** 204, 2011.

199. Peak, C.W., Singh, K.A., Adlouni, M.a., Chen, J., and Gaharwar, A.K. Printing therapeutic proteins in 3D using nanoengineered bioink to control and direct cell migration. Adv Healthc Mater **8,** 1801553, 2019.

200. Cross, L.M., Carrow, J.K., Ding, X., Singh, K.A., and Gaharwar, A.K. Sustained and prolonged delivery of protein therapeutics from two-dimensional nanosilicates. ACS Appl Mater Interfaces **11,** 6741, 2019.

201. Sydney Gladman, A., Matsumoto, E.A., Nuzzo, R.G., Mahadevan, L., and Lewis, J.A. Biomimetic 4D printing. Nat Mater **15,** 413, 2016.

202. Zarek, M., Mansour, N., Shapira, S., and Cohn, D. 4D printing of shape memory-based personalized endoluminal medical devices. Macromol Rapid Commun **38,** 1600628, 2017.

203. Zarek, M., Layani, M., Cooperstein, I., Sachyani, E., Cohn, D., and Magdassi, S. 3D printing of shape memory polymers for flexible electronic devices. Adv Mater **28,** 4449, 2016.

204. Mulakkal, M.C., Trask, R.S., Ting, V.P., and Seddon, A.M. Responsive cellulose-hydrogel composite ink for 4D printing. Mater Des **160,** 108, 2018.

205. Baker, A.B., Bates, S.R.G., Llewellyn-Jones, T.M., Valori, L.P.B., Dicker, M.P.M., and Trask, R.S. 4D printing with robust thermoplastic polyurethane hydrogel-elastomer trilayers. Mater Des **163,** 107544, 2019.

206. Ge, Q., Qi, H.J., and Dunn, M.L. Active materials by four-dimension printing. Appl Phys Lett **103,** 131901, 2013.

207. Das, S., Kim, S.W., Choi, Y.J., *et al.* Decellularized extracellular matrix bioinks and the external stimuli to enhance cardiac tissue development in vitro. Acta Biomater **95,** 188, 2019.

208. DeForest, C.A., and Tirrell, D.A. A photoreversible protein-patterning approach for guiding stem cell fate in three-dimensional gels. Nat Mater **14,** 523, 2015.

209. Shadish, J.A., Benuska, G.M., and DeForest, C.A. Bioactive site-specifically modified proteins for 4D patterning of gel biomaterials. Nat Mater **18,** 1005, 2019.

210. Guillotin, B., and Guillemot, F. Cell patterning technologies for organotypic tissue fabrication. Trends Biotechnol **29,** 183, 2011.

211. Forgacs, G. Tissue engineering perfusable vascular networks. Nat Mater **11,** 746, 2012.

212. Duan, B., Kapetanovic, E., Hockaday, L.A., and Butcher, J.T. Three-dimensional printed trileaflet valve conduits using biological hydrogels and human valve interstitial cells. Acta Biomater **10,** 1836, 2014.

213. Rezende, R.A., Bartolo, P.J., Mendes, A., and Maciel, R. Rheological behavior of alginate solutions for biomanufacturing. J Appl Polym Sci **113,** 3866, 2009.

214. Skardal, A., Zhang, J., and Prestwich, G.D. Bioprinting vessel-like constructs using hyaluronan hydrogels crosslinked with tetrahedral polyethylene glycol tetracrylates. Biomaterials **31,** 6173, 2010.

215. Rhee, S., Puetzer, J.L., Mason, B.N., Reinhart-King, C.A., and Bonassar, L.J. 3D Bioprinting of spatially heterogeneous collagen constructs for cartilage tissue engineering. ACS Biomater Sci Eng **2,** 1800, 2016.

216. Obara, K., Ishihara, M., Ishizuka, T., *et al.* Photocrosslinkable chitosan hydrogel containing fibroblast growth factor-2 stimulates wound healing in healing-impaired db/db mice. Biomaterials **24,** 3437, 2003.

217. Khattak, S.F., Spatara, M., Roberts, L., and Roberts, S.C. Application of colorimetric assays to assess viability, growth and metabolism of hydrogel-encapsulated cells. Biotechnol Lett **28,** 1361, 2006.

218. Cheng, Y.-H., Yang, S.-H., Su, W.-Y., *et al.* Thermosensitive chitosan–gelatin–glycerol phosphate hydrogels as a cell carrier for nucleus pulposus regeneration: an in vitro study. Tissue Eng Part A **16,** 695, 2009.

219. Ribeiro, M., Morgado, P., Miguel, S., Coutinho, P., and Correia, I. Dextran-based hydrogel containing chitosan microparticles loaded with growth factors to be used in wound healing. Mater Sci Eng C **33,** 2958, 2013.

220. Balestrin, L., Bidone, J., Bortolin, R., Moresco, K., Moreira, J., and Teixeira, H. Protective effect of a hydrogel containing Achyrocline satureioides extract-loaded nanoemulsion against UV-induced skin damage. J Photochem Photobiol B Biol **163,** 269, 2016.

221. e Silva, S.A.M., Calixto, G.M.F., Cajado, J., *et al.* Gallic acid-loaded gel formulation combats skin oxidative stress: development, characterization and ex vivo biological assays. Polymers (Basel) **9,** pii: E391, 2017.

222. Mahoney, M.J., and Anseth, K.S. Three-dimensional growth and function of neural tissue in degradable polyethylene glycol hydrogels. Biomaterials **27,** 2265, 2006.

223. Galateanu, B., Dimonie, D., Vasile, E., Nae, S., Cimpean, A., and Costache, M. Layer-shaped alginate hydrogels enhance the biological performance of human adipose-derived stem cells. BMC Biotechnol **12,** 35, 2012.

224. Suri, S., and Schmidt, C.E. Cell-laden hydrogel constructs of hyaluronic acid, collagen, and laminin for neural tissue engineering. Tissue Eng Part A **16,** 1703, 2010.

225. Lu, J., He, Y.S., Cheng, C., *et al.* Self-Supporting graphene hydrogel film as an experimental platform to evaluate the potential of graphene for bone regeneration. Adv Funct Mater **23,** 3494, 2013.

226. Saladino, S., Di Leonardo, E., Salamone, M., Mercuri, D., Segatti, F., and Ghersi, G. Formulation of different chitosan hydrogels for cartilage tissue repair. Chem Eng Trans **38,** 505, 2014.

227. Devine, D.M., Devery, S.M., Lyons, J.G., Geever, L.M., Kennedy, J.E., and Higginbotham, C.L. Multifunctional polyvinylpyrrolidinone-polyacrylic acid copolymer hydrogels for biomedical applications. Int J Pharm **326,** 50, 2006.

228. Yin, L., Zhao, X., Cui, L., *et al.* Cytotoxicity and genotoxicity of superporous hydrogel containing interpenetrating polymer networks. Food Chem Toxicol **47,** 1139, 2009.

229. Oliveira Barud, H.G., Barud Hda, S., Cavicchioli, M., *et al.* Preparation and characterization of a bacterial cellulose/silk fibroin sponge scaffold for tissue regeneration. Carbohydr Polym **128,** 41, 2015.

230. Peng, Z., and Shen, Y. Study on biological safety of polyvinyl alcohol/collagen hydrogel as tissue substitute (I). Polym Plast Technol Eng **50,** 245, 2011.

231. Park, S.A., Lee, S.H., and Kim, W.D. Fabrication of porous polycaprolactone/hydroxyapatite (PCL/HA) blend scaffolds using a 3D plotting system for bone tissue engineering. Bioprocess Biosyst Eng **34,** 505, 2011.

232. Fielding, G.A., Bandyopadhyay, A., and Bose, S. Effects of silica and zinc oxide doping on mechanical and biological properties of 3D printed tricalcium phosphate tissue engineering scaffolds. Dent Mater **28,** 113, 2012.

233. Du, H., Hamilton, P., Reilly, M., and Ravi, N. Injectable in situ physically and chemically crosslinkable gellan hydrogel. Macromol Biosci **12,** 952, 2012.

234. Debnath, T., Ghosh, S., Potlapuvu, U.S., *et al.* Proliferation and differentiation potential of human adipose-derived stem cells grown on chitosan hydrogel. PLoS One **10,** e0120803, 2015.

235. Teong, B., Lin, C.-Y., Chang, S.-J., *et al.* Enhanced anti-cancer activity by curcumin-loaded hydrogel nanoparticle derived aggregates on A549 lung adenocarcinoma cells. J Mater Sci Mater Med **26,** 49, 2015.

Address correspondence to:
Akhilesh K. Gaharwar, PhD
Department of Biomedical Engineering
College of Engineering
Texas A&M University
College Station, TX 77843

E-mail: gaharwar@tamu.edu